Phase-Specific Stiffness of Sprinting Prostheses

G.J. van der Gun

Technische Universiteit Delft

TUDelft

Phase-Specific Stiffness of Sprinting Prostheses

Performance Enhancement of Amputee Sprinting: A Modelling Approach

by

G.J. van der Gun

to obtain the degree of Master of Science
at the Delft University of Technology,
to be defended on Thursday November 22, 2018 at 10:00.

Student number:	4512235	
Project duration:	March, 2018 – November, 2018	
Thesis committee:	Dr. Ir. A. L. Schwab,	TU Delft 3mE/BmechE, chair
	Dr. D. J. J. Bregman,	TU Delft 3mE/BmechE, daily supervisor
	Dr. B. Shyrokau,	TU Delft 3mE/COR, member
	Dr. Ir. O. K. Bergsma,	TU Delft LR/ASM, member

An electronic version of this thesis is available at http://repository.tudelft.nl/.

TU Delft

Abstract

Running-specific prostheses enable amputee athletes to perform at the highest level. However, current prosthesis design still impairs sprinting performance in multiple ways. An example is the constant mechanical stiffness of the prosthetic devices. The dynamic behaviour of the blade is determined by this property, but it is static and cannot change according to the gait phase-specific sprinting dynamics. During acceleration a different stiffness might be required as opposed to steady state running. Therefore, it is hypothesised that amputee athletes can improve their performance with prostheses that have a gait phase-specific stiffness.

In order to investigate the effect of stiffness on amputee sprinting performance a novel and unprecedented modelling approached is used. Modelling is economical and straightforward in comparison to other research methods such as laboratory experiments. In this thesis, an extension of the established Spring-Loaded Inverted Pendulum model is proposed that qualitatively describes amputee sprinting motion. The Actuated Spring-Loaded Inverted Pendulum (ASLIP) is capable of predicting stable forwardly integrated sprinting motion with the inclusion of the start and acceleration phase. Optimisation of the model predicts that phase-specific spring stiffness leads to a significant time reduction on the 100m sprint for given physiological parameters. In general it can be said that a stiffer spring results in better performance. More specifically, the model benefits from a stiff spring during acceleration and a more compliant one in steady state. Although it has its limitations, the ASLIP model additionally provides a valuable insight into the mechanics of amputee sprinting. For example, it seems that optimal phase-specific stiffness is strongly dependent on biomechanical parameters such as touchdown angle, force angle and CoM velocity. Future work in this direction can provide a better understanding of the underlying mechanisms that determine amputee sprinting performance.

The outcomes of this study suggest that amputee sprinters might be able to achieve a reduction in finishing time with prosthetic devices that have a phase-specific stiffness. The modelling approach used in this thesis is promising and lends itself well to investigate this opportunity in more detail.

Preface

> Victorious warriors win first and then go to war, while defeated warriors go to war first and then seek to win.
>
> Sun Tzu, *The Art of War*

This report is the result of my master thesis, the final step in completing the master Biomedical Engineering of the TU Delft. The topic of this project came about in conversations with one of my supervisors, Daan Bregman, earlier this year. I owe to him the smooth initiation of my project. I would like to thank him and Arend Schwab for their time and skilled advice throughout my research. Your relaxed manner of guidance suits me and you knew when to motivate me to work hard if it was needed. I would like to further thank the people of Haag Atletiek and the Dutch Para Athletics Team for their collaboration. In particular Arno Mul and his athletes. The results that I got out of the cooperation with them mark an important part of my research.

G.J. van der Gun
Delft, November 2018

Contents

List of Figures

List of Tables

List of Abbreviations

A	Aerial phase
ABS	Able-Bodied Sprinting
AS	Amputee Sprinting
ASLIP	Actuated Spring-Loaded Inverted Pendulum
CA	Active Contact phase
CP	Passive Contact phase
CoM	Centre of Mass
Fstep	Step frequency
GCP	Ground Contact Point
GRF	Ground Reaction Force
IPC	International Paralympic Committee
Lstep	Step length
RSP	Running-Specific Prostheses
SLIP	Spring-Loaded Inverted Pendulum

1 Introduction

Paralympic sports are growing more popular. Next to dedication and hard work of the athlete, technology plays a significant role in enabling athletes with an impairment to perform at the highest level. More than able-bodied athletes, amputee athletes make use of technological advancements to increase their performance. For example, amputee sprinters performing in the 100m sprint make use of running-specific prostheses. These carbon blades have energy storage and return capabilities that have enabled the athletes to achieve a running gait that is biomechanically similar to able-bodied athletes. Since the introduction of the blades, amputee sprinting has seen an exceptionally large increase in performance. Nonetheless, amputee sprinters are still second to their able-bodied colleagues.

One of the reasons for this might be that current prosthesis design impairs amputee sprinting performance. It is known that stiffness of the running blades has an influence on performance [1–5]. Among other mechanical properties, stiffness governs the dynamic behaviour of the blade. With parameters such as composition, shape or form of the composite material this behaviour can be 'designed' for its intended function. The International Paralympic Committee has set requirements regarding sports equipment [6]. However, they do not exclude the use of these parameters to improve design and potentially make blade runners faster.

Amputee athletes can benefit from gait phase-specific mechanical behaviour of sprinting prostheses. Modern blades are designed to mimic the function of biological legs. They work as a spring: storing and releasing energy during the contact phase. One of the main differences is that humans can modulate leg stiffness by contracting muscles but the mechanical stiffness of the blade remains constant. This might not be a problem in steady state running, under the assumption that there is no change in motion of the sprinter in that phase. However, the dynamics of the acceleration phase of the 100m sprint do seem to require a more variable solution. In particular because this phase is relatively long in comparison to other race distances and thus crucial for the end result. For that reason, it is desirable to investigate the effect of phase-specific stiffness on amputee sprinting performance.

The current methods used to design running-specific prostheses fail to effectively qualify the optimal mechanical behaviour of running blades. Laboratory experiments are the golden standard for quantifying these properties and their effect on sprinting performance. This method is costly and only the effect of a single property on overall performance can be reliably tested. The interdependency of many of the biomechanical parameters as well as the mechanical properties ask for a more convenient way of testing.

A suitable method for finding the optimal phase-specific stiffness of running prostheses is modelling. Forward dynamic modelling is a simple way of simulating amputee sprinting and its results can be relatively easily validated. The spring-mass model for running and hopping is an example of a dynamic model that has been shown to accurately simulate human running [7]. More importantly, it is suitable for the addition of active elements in order to model start and acceleration. Furthermore, the structure of the model enables the use of numerical optimisation methods. The use of a forward dynamic model as a tool in the design of running-specific prostheses is promising and without precedent in literature.

It is hypothesised that the current prostheses design can be improved by introducing gait phase-specific stiffness to achieve faster sprinting times. The purpose is to find a conceptually optimal phase-specific stiffness of sprinting prostheses, using a forward dynamic model of amputee sprinting. The

following research question is formulated:

Can phase-specific stiffness of sprinting prostheses enhance performance of amputee athletes in the 100m sprint?

An extension of the well established simple spring-mass model is used to investigate what mechanisms are responsible for amputee sprinting performance and how these are interrelated. With the help of numerical optimisation methods an optimal phase-specific stiffness is calculated. The extension of the forward dynamic model will be validated with physical motion data. The outline of the thesis report is as described below.

A literature study was performed preceding this thesis. The findings of this study that are relevant to the work presented in this report can be found in Chapter 2. In Chapter 3 it is demonstrated that the simple spring-mass model describes human running well. Furthermore, an active extension to this spring-mass model is proposed that is capable of simulating amputee sprinting including start and acceleration. Chapter 4 focuses on the optimisation of the proposed model and presents an optimal phase-specific stiffness. The validity of the results is discussed in Chapter 5. An answer to the research question is provided in Chapter 6.

2

Background

Since the introduction of Running-Specific Prostheses (RSP) amputee athletes have drastically improved their sprinting performance. The men's 100m winning times at the Paralympic games in the T43/T44 (or comparable) class went from 13.12 s in 1984 to 11.73 in 1988 (see Figure 2.1). This is an exceptionally large increase in performance that is greater than what has been observed for Olympic athletes and Paralympic athletes from other classes [8]. The dynamic behaviour of modern RSP's mimics that of human legs. It is assumed that the increase in sprinting performance of amputee sprinters (AS) is mainly due to this. The spike in AS performance has attenuated in recent years [9], but it is not hard to imagine that new revolutionary technological advancements induce another AS performance spike, similar to what happened in 1984 to 1988. The (bio)mechanics of sprinting need to be understood in order to find out.

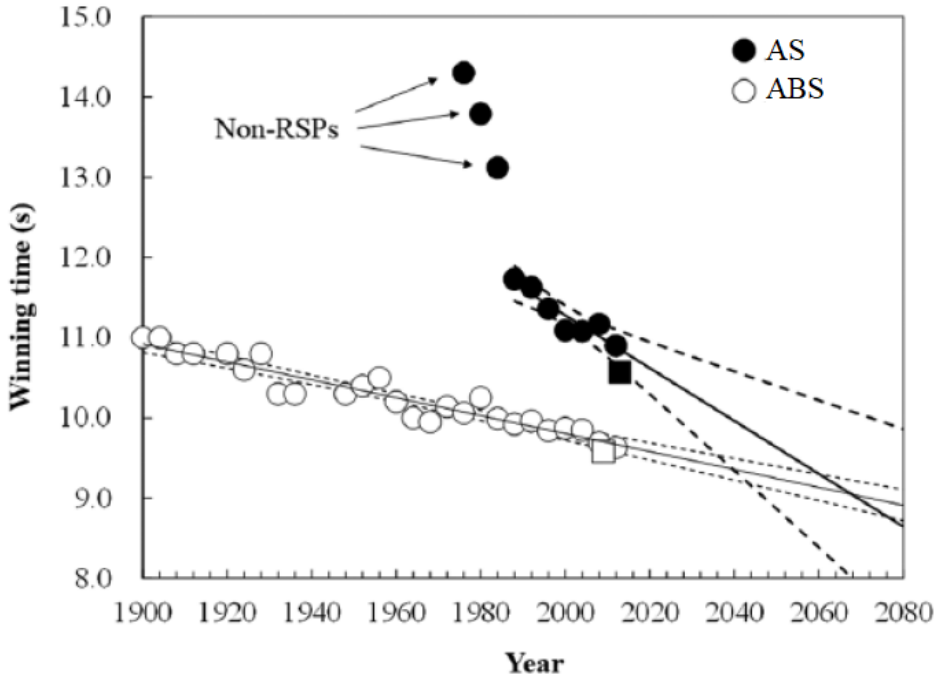

Figure 2.1: Men's 100m winning time of AS (unfilled circles) and ABS (filled circles) throughout the years. The solid lines are linear regression lines. Taken from [10].

2.1. Biomechanics of Sprinting

The motion of a human leg during sprinting can be seen as a cycle of two alternating phases: the stance or contact phase and the swing or aerial phase (Figure 2.2). During the contact phase the foot is in contact with the ground. In this phase the shock of impact is absorbed and the force is produced that propels the athlete forward. The aerial phase follows after the stance phase and starts and ends with a double float where both legs are in the air. During the aerial phase the leg is repositioned ('swung') in front of the runner to start a new cycle [11]. The contact phase is were most forces act on the runner. This phase is essential for the acceleration that characterises sprint running.

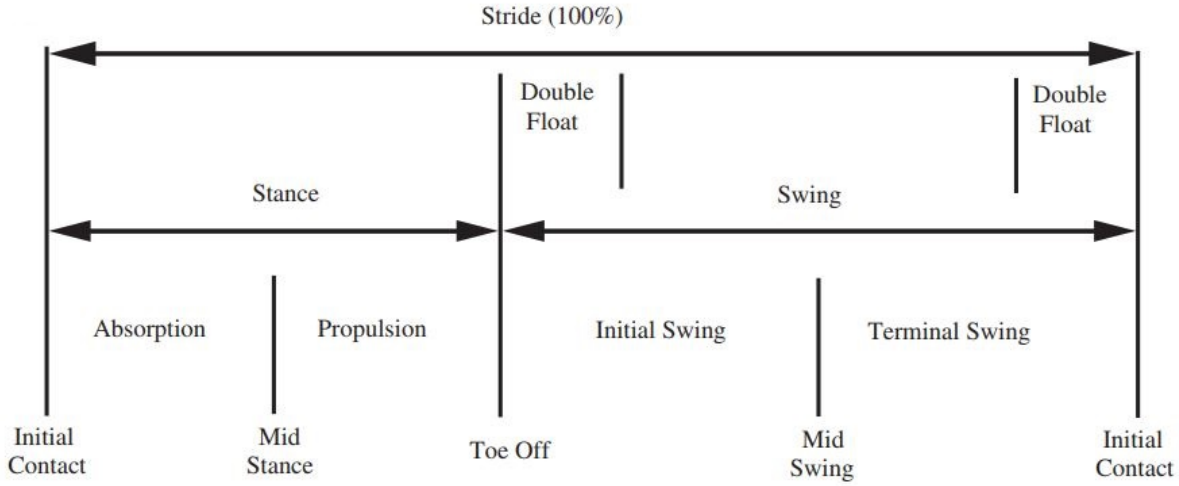

Figure 2.2: Running gait consists of two phases: stance phase and swing phase. Taken from [11].

Acceleration and start are crucial stages of the 100m sprint. Sprint running is characterised by a relatively long acceleration stage. The shorter the distance the more important this stage is for overall performance. Figure 2.3 shows the velocity throughout the race of the three fastest 100m sprints of Usain Bolt. It can be seen that top speed is reached only at around 75% of the total distance. Top performance in sprinting distances is therefore often signified by fast starting and high acceleration [12, 13]. From a mechanical perspective these stages of the race are interesting as well: because acceleration is a dynamic process they require the athlete to adapt their behaviour.

The biomechanics of amputee athletes are not fundamentally different than able-bodied athletes. Both ABS and AS have extensor muscles that act across the knee and hip during running at constant speed [15]. Kinetic energy is stored in these muscles and their tendons during the start of the stance phase and released towards the end [7, 14, 16, 17]. The legs of sprinters act as a spring-like mechanism during running. The difference in lower limb mechanics do not signify a different sprinting physiology altogether. Accordingly, kinematic variables that are related to sprinting performance in able-bodied sprinters might also have a similar relationship for impaired athletes. In no particular order, the important biomechanical parameters of sprinting are:

- Leg stiffness (Kleg)
- Step frequency (Fstep)
- Step length (Lstep)
- Contact time (Lcon)
- Ground Reaction Force (GRF)

High speeds are associated with the ability to produce a strong forward impulse, i.e. large forces, in a short amount of time. In other words, a powerful athlete that is able to achieve a high step frequency, with a short contact time and a (relatively) long step length will perform well in the 100m sprint [18–20]. The rules and regulations of the IPC dictate that all energy that is stored in the prosthetic device

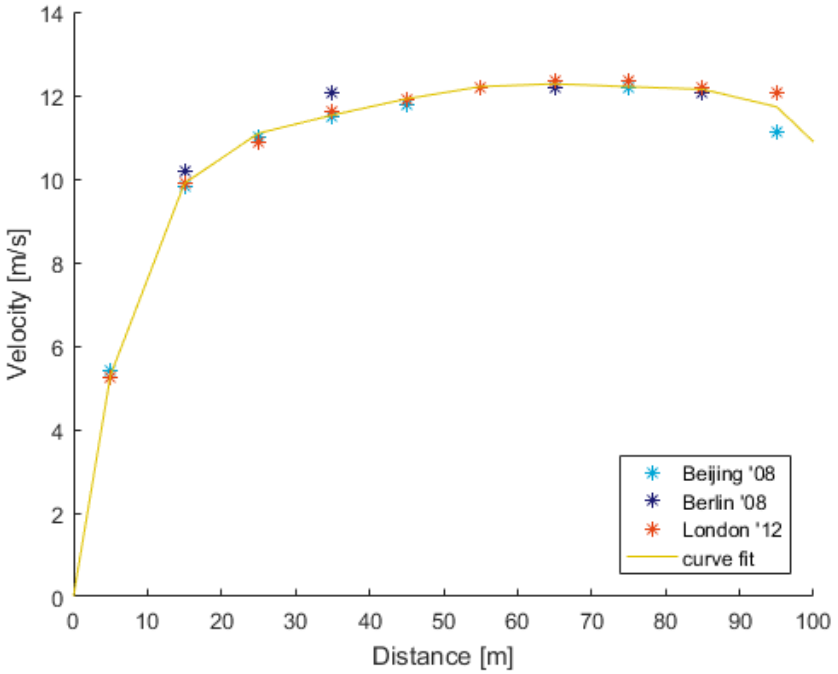

Figure 2.3: The mean 10m interval velocity of Usain Bolt's three best 100m sprints: Beijing 2008, Berlin 2009 (Current World Record) and London 2012 (Current Olympic Record). A 4^{th} order polynomial is fitted over the data points. Data retrieved from [14].

must be generated during the race by the athlete [6]. For this reason, active elements are not allowed. Increasing the propulsive forces can therefore not be made an engineering challenge. However, the spatiotemporal variables Lstep, Fstep and Lcon can be influenced by leg stiffness [2, 15].

Of these biomechanical parameters, stiffness is one of the most significant determinants for sprinting performance. Already in the seventies it was discovered that track stiffness could enhance running speed [21]. A special running track was built at Harvard University that is believed to produce a speed enhancement of 2% (many records were ran there). In a way, this track can be seen as a 'prosthetic device' and it proofs that tuning stiffness can indeed enhance performance. Many studies have shown that Kleg correlates significantly with amputee sprinting ability [1, 2, 4, 22, 23]. Thus, next to the direct influence stiffness has on other spatiotemporal parameters it is an important factor of sprint performance on its own as well. This may be an opportunity to improve amputee sprinting performance.

2.2. Mechanical properties of Running-Specific Prostheses

Modern RSP's are designed to mimic the function of biological legs. The blades work as a spring: storing and releasing energy during the contact phase. Kinetic energy is stored in the blade in the form of potential energy [20]. At initial contact the downwards velocity of the Centre of Mass (CoM) of the athlete compresses the RSP blades ('absorption', see Figure 2.2). At toe-off the blade returns to its original shape and energy is partially returned to the sprinter (Figure 2.4). During steady state running, this energy exchange is very effective because the return is more forwardly oriented, accelerating the sprinter. However, during acceleration the stance leg of the athlete is placed almost directly under the CoM. Therefore, the storage of kinetic energy is minimal. In this case, a compliant blade is disadvantageous as it damps out the force produced by the athlete, impairing acceleration.

Current RSP's have constant mechanical properties that might not be optimal for the dynamic acceleration stage. Able-Bodied Sprinters (ABS) can change the mechanical properties of their legs by contracting their muscles [2, 22, 24]. However, the mechanical properties of the blade are static; they cannot change over the course of the race. In addition, AS are not able to modulate their leg stiffness as much as ABS. The perceived stiffness of athletes using RSP's is therefore heavily influenced by the dynamic behaviour of their RSP's. Many studies have investigated the effect of RSP properties

on steady state running [25–27], but few relate these to accelerating performance. Currently, stiffness of a sprinting prosthesis is optimised for steady state running at top speed. Therefore, it might impair acceleration and start performance of amputee athletes. This is in accordance to what is reported by amputee athletes themselves. In an interview, two-time T43 Paralympic Champion and T43 World Champion Marlou van Rhijn, has said that she notices that in the start the blade first 'damps' out the energy she produces and that it takes too long for the blade to return this energy. She has the feeling that it impairs her starting performance.

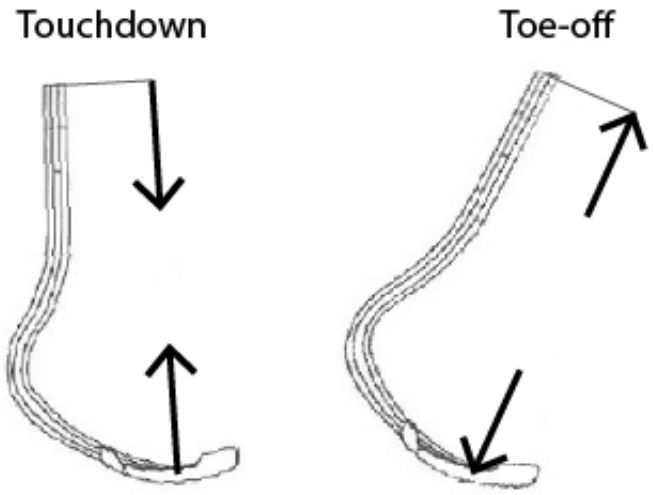

Figure 2.4: The working principle of carbon fibre RSP blades: energy storage and return during the contact phase.

Amputee athletes might benefit from phase-specific mechanical properties of RSP's. In theory a rigid blade would lead to the fastest acceleration: the generated propulsive force is instantaneously transferred into forward velocity. However, apart from the first step out of the starting block, an amputee sprinter is never able to stably provide a completely forwardly oriented GRF. During acceleration the spatiotemporal parameters change every step. This requires athletes to adjust leg stiffness over a wide range in order to achieve optimal performance [24, 28]. The constant mechanical properties of RSP's are a limiting factor for AS. They can therefore possibly benefit from a prosthesis that is stiffer at the start and becomes more compliant towards the end of the acceleration. With the design possibilities of carbon fibre reinforced polymers, running-specific prostheses that have such properties could be developed. These prostheses would enable athletes to benefit from both the direct transfer of propulsive forces into forward velocity during start and acceleration as well as the efficient energy storage and release capabilities during steady state running.

3

Modelling Amputee Sprinting

In the previous chapter it is hypothesised that the current prostheses design can be improved by introducing phase specific properties to achieve faster running times, especially in the sprint distance. Laboratory experiments are currently the golden standard for quantifying these properties and their effect on sprinting performance. Generally, only the effect of a single property on overall performance can be reliably tested. The interdependency of many parameters and properties of sprinting and sprinting prostheses imply that an optimum is not easily found. Furthermore, the problem is to optimise not only for maximum sprinting velocity but also for all speeds proceeding because the athlete spends a significant part of the race accelerating. Attempting to solve this problem with experiments only would be a laborious and costly process.

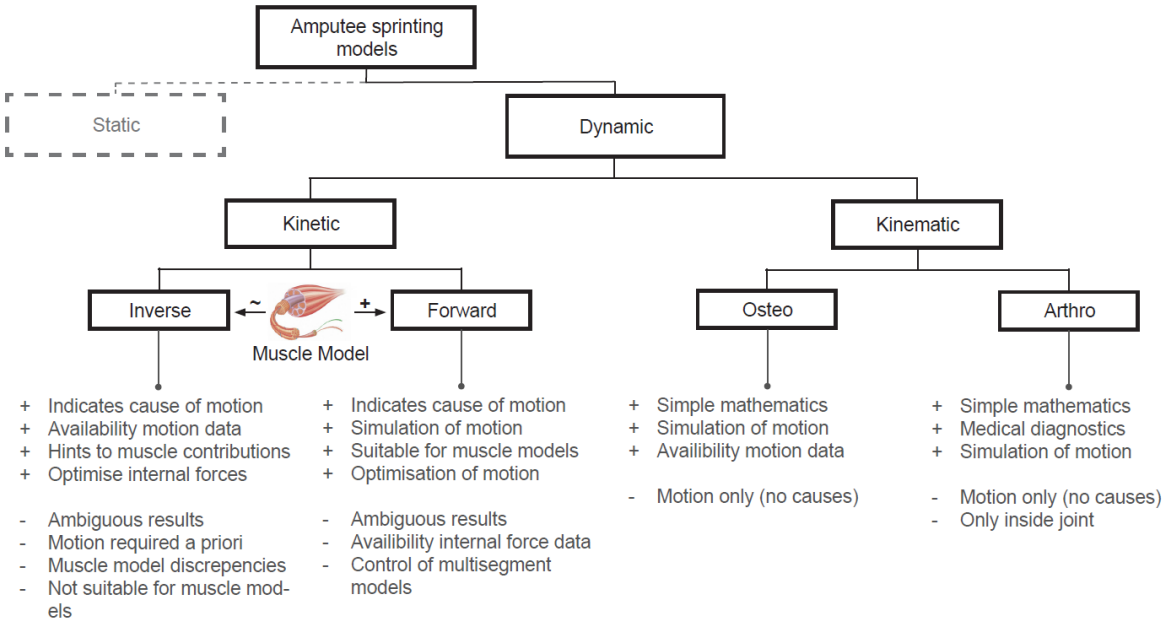

Figure 3.1: Schematic overview of the available dynamic model types and some examples.

A suitable method for finding the optimal phase specific properties of running prostheses can be modelling. There are many different modelling methods which all have their considerations (see Figure 3.1). Forward dynamic modelling is capable of simulating amputee sprinting, its results can be relatively easily validated, it provides means to investigate causes of motion and it enables the use of numerical optimisation methods. With these methods, a range of optimal phase-specific mechanical properties given a set of physiological parameters can be calculated quickly and easily. Furthermore, no athletes need to be involved. In this way, an indication of what to test for in the laboratory can be made,

possibly saving money, time and effort of scientists and athletes. This approach is promising and without precedent in literature.

An example of a simple dynamic model that is capable of simulating human running is the spring-mass model for running and hopping [7]. It has been shown repeatedly that this model describes human running exceptionally well [28, 29] and its use is well established in sports science. It is a forward dynamic model which has segment motion as output. It is therefore particularly useful to investigate the effect of mechanical properties on sprinting velocity and/or finishing time. The next section is dedicated to discuss the the spring-mass model in more detail.

3.1. Spring-Loaded Inverted Pendulum

The spring-mass model for running and hopping is a widely recognised as a qualitative representation of the running gait of a human because of its energy conservation properties. The model is also known as the Spring-Loaded Inverted Pendulum (SLIP): it consists of a point mass attached to a massless spring. The model structure is based on the assumption that a human musculoskeletal system is mechanically very similar to a multicomponent, non-linear spring-mass system that is actively driven. This is simplified further by assuming that for certain running and hopping frequencies the legs of humans can be approximated by a simple bouncing system without viscous losses. The original planar model is shown in Figure 3.2. Just as human running has two alternating phases the SLIP model consists of two alternating sets of motion equations for the contact and aerial phase respectively:

Contact phase:

$$\ddot{x} = \frac{k}{m}(l_0 - l_s)\cos(\alpha) \tag{3.1}$$

$$\ddot{y} = \frac{k}{m}(l_0 - l_s)\sin(\alpha) - g \tag{3.2}$$

Aerial phase:

$$\ddot{x} = 0 \tag{3.3}$$

$$\ddot{y} = -g \tag{3.4}$$

with

$$l_s = \sqrt{{x_l}^2 + y^2} \tag{3.5}$$

$$x_l = l_s \cos\alpha \tag{3.6}$$

and x, y the coordinates of the Centre of Mass (CoM), m the mass of the athlete, α angle of the leg, k the stiffness of the spring, g the gravitational acceleration and l_s the spring length with resting spring length l_0. The x-position of the Ground Contact Point (GCP) is defined as $X_{GCP} = x + x_l$.

The instantaneous leg angle at initial contact α_i (or touchdown angle) is constant over all steps and is known a priori. The solver switches to the contact equations of motion as soon as the y-position of the CoM is equal to the y-component of the resting spring length $y = y_{s_0}$. The solver switches back to the aerial equations when the resting spring length l_{s_0} is reached again (see Figure 3.3 and Equations 3.1-3.4). It is assumed that there are no viscous losses at heel-strike and no aerodynamic drag. The configuration of the model at any point is described by the coordinates of the CoM x, y and leg angle α. The gravitational force field g is directed in the negative y-direction.

3.1.1. Analysis of the SLIP Model

Simulating the runners motion consists of integrating the equations of motion using the ODE45 solver in Matlab (see Appendix C). The model is started in the air with initial position $x_0 = 0\ m$ and $y_0 = 0.9\ m$. The leg angle at initial contact is set to $\alpha_i = 125°$ for every step. The physical constants are: mass $m = 64\ kg$, resting spring length $l_{s_0} = 0.9\ m$ and gravitational acceleration $g = 9.81\ ms^{-2}$. Stiffness was increased from 10 kNm^{-1} at 3 ms^{-1} to 30 kNm^{-1} at 9 ms^{-1} in accordance with the range of reported values in literature [16, 24, 25, 30]. With these parameters the model settles into a stable, repeated stride pattern for a range of common running velocities. Table 3.1 shows the output of the model for

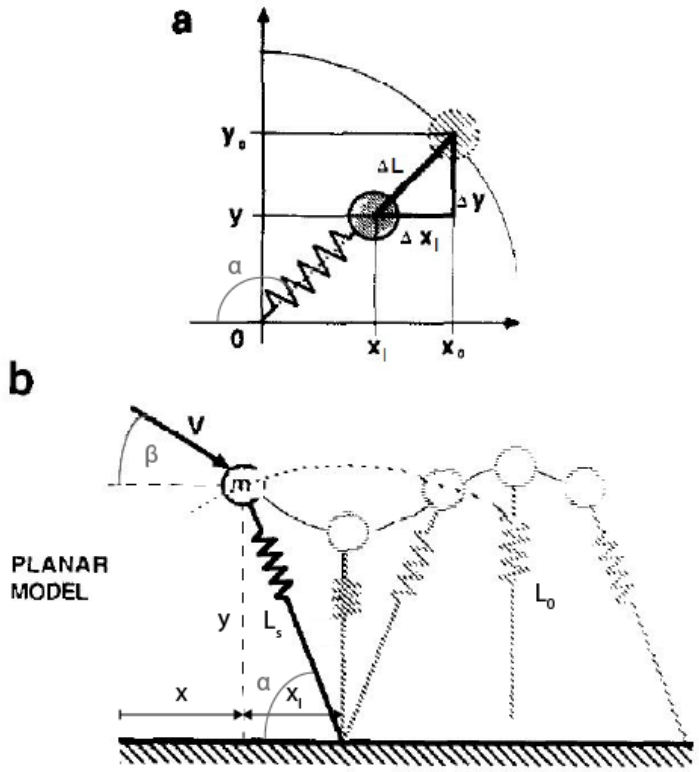

Figure 3.2: The spring-mass model for running. **A.** The spring length l can be subdivided into vertical and horizontal components using angle α. The horizontal component is the local x-position of the CoM. **B.** The velocity of the point mass is a vector which direction is determined by angle β. The x-position of the ground contact point is $X_{GCP} = x + x_l$. Taken from [7].

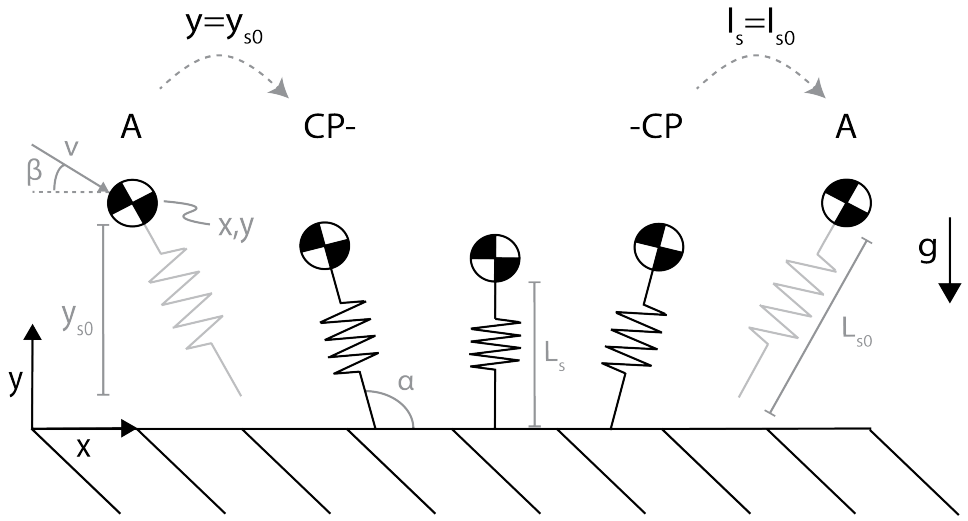

Figure 3.3: A schematic overview of the operation of the SLIP model: the solver switches from aerial to contact equations when the y-position of the CoM is equal to the y-component of the resting spring length. The contact phase ends when the spring has returned to its resting length and the solver switches back to the aerial equations (see also Equations 3.1-3.4).

Input	$v\ [ms^{-1}]$	3	5	7	9
	$k\ [kNm^{-1}]$	10	17	24	30
	$\alpha_i\ [deg]$	25	25	25	25
	$\beta_0\ [deg]$	5	5	5	5
Output	$L_{step}\ [m]$	1.29	1.41	1.66	1.94
	$F_{step}\ [Hz]$	2.1	2.3	2.9	3.4
	$F_{y_{max}}\ [BW]$	3.22	4.41	4.95	5.56
	$T_{con}\ [s]$	0.243	0.159	0.111	0.086

Table 3.1: Output of the Spring-Loaded Inverted Pendulum model for different speeds and stiffnesses. The found values are physiologically common. BW stands for bodyweight.

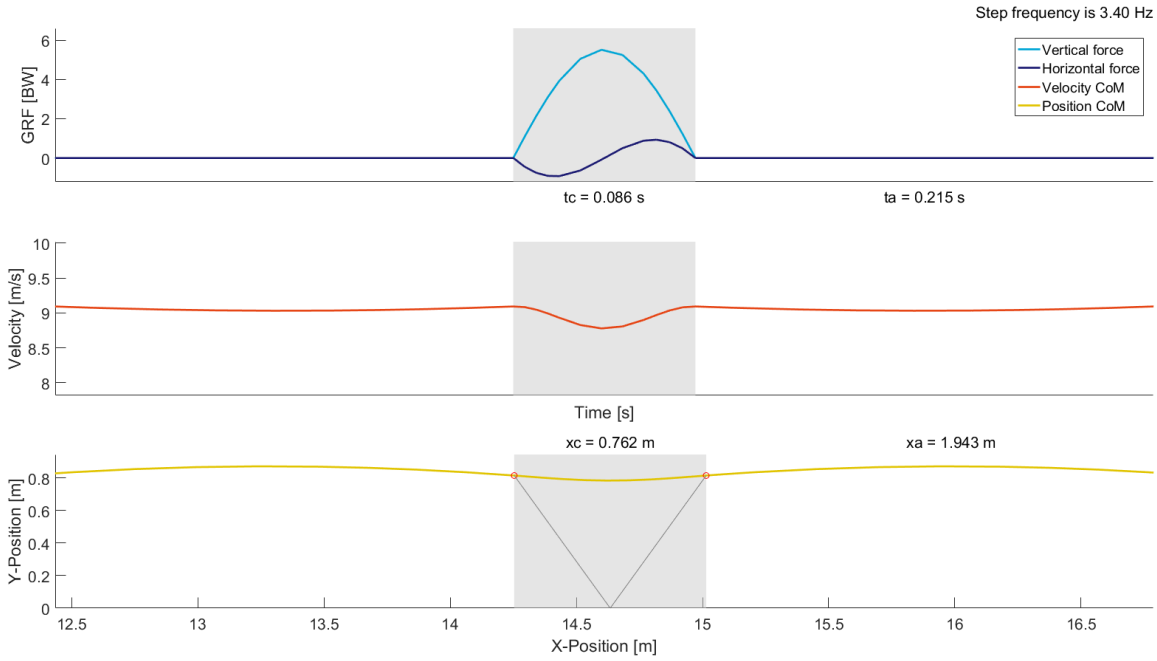

Figure 3.4: Output of one step of the simulated Spring-Loaded Inverted Pendulum model with initial conditions $x_0 = 0\ m$, $y_0 = 0.9\ m$, $v_0 = 9\ ms^{-1}$ and $\beta_0 = 5°$. The leg angle at initial contact is set to $\alpha_i = 125°$ for every step. Leg stiffness $k = 30\ kNm^{-1}$. The simulated motion describes human running well.

different velocities and stiffnesses. The simulated motion, CoM velocity and GRF's for one step of the SLIP model are plotted in Figure 3.4.

The Spring-Loaded Inverted Pendulum model of Blickhan describes human running well. Step frequency and peak vertical GRF of the model range from 2.1 Hz and approximately 3 times bodyweight (BW) at 3 ms^{-1} to 3.4 Hz and approximately 5.5 BW at 9 ms^{-1}. This as well as the step length produced by the model is physiologically common at these speeds [14, 19, 31]. The chosen stiffnesses and touchdown angles allow for close to horizontal velocity angle and this results in a low vertical displacement of the CoM. The same smooth motion pattern is observed in human running [2, 31]. Although the model is not a quantitative description of running, it can be concluded that the Spring-Loaded Inverted Pendulum behaves very similarly to the active bouncing system that a human runner is.

Despite that the SLIP model can be used to simulate steady state running, it is not capable of describing start and acceleration that are crucial for sprinting. The validity of the model must not be overstated, it has its limitations. For instance, humans can actively apply forces to accelerate. Even during running in steady state a higher take-off than landing velocity is observed [7]. The SLIP model assumes a similar take-off and landing velocity and is therefore not capable of simulating any kind of acceleration. In addition, the model does not take into account the conservation of momentum in the

swing phase due to the mass of the distal leg, it assumes complete symmetry across the sagittal plane and it neglects the influence of other moving masses in the body. In order to investigate the effect of RSP stiffness on sprinting performance, additions to the SLIP model need to be made.

3.2. Motion Analysis of Amputee Sprinting

Detailed and complete motion data of amputee sprinters is scarce in literature, but indispensable for the extension of existing running models. The CoM trajectory of amputee sprinters during of the total 100m sprint have not been directly obtained in other studies. For the simulation some input parameters (e.g. touchdown angle α_i per step) are required beforehand. Moreover, it is paramount that any additions to the spring-mass model are validated before conclusions are drawn from its results. Namely, the output of the model should be directly compared to actual data. In order to retrieve this data it was decided to film amputee athletes during a 100m sprint and do a motion analysis on the resulting images.

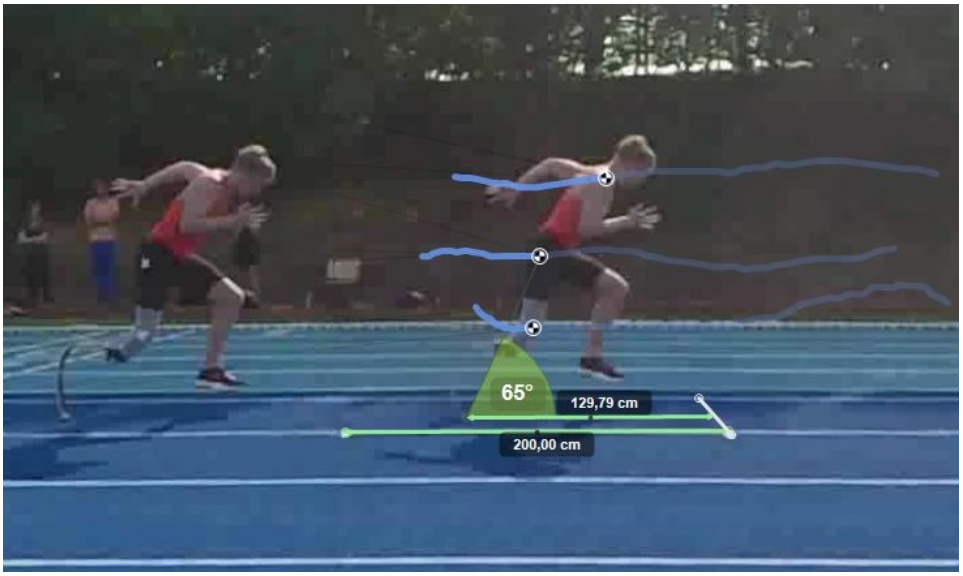

Figure 3.5: An example image of motion analysis performed with Kinovea on the athletes. Raw trajectory data, angles and distances were further processed using Matlab.

The participants were three transtibial unilateral (two left, one right-sided) amputee sprinters of TeamNL at Papendal. They are elite athletes specialising in the sprint and long jump disciplines. Each subject performed two 100m sprints with maximal acceleration from a block start. The motion was recorded from the side with eight cameras on tripods positioned alongside the track. The images of the cameras overlapped so that the whole 100m from start to finish was captured. Before each start all cameras were synchronised so that the videos could later be combined. The cameras had a minimum frame rate of 60 fps and a resolution of 720p. The start and acceleration until 30m were captured with a minimum of 120 fps in full HD. Horizontal distance markers were applied on the track every two metres so that measurements could be calibrated. A diagram of the camera setup can be found in Appendix A. The acromion, trochanter and lower epicondyle of the athlete's side that was closest to the camera were marked using white tape. An example of a camera image and motion analysis is shown in Figure 3.5.

With motion analysis software Kinovea, the angles, distances and times could be measured. The trajectory of the marked bony landmarks was tracked using the built-in tracking software. Two runs were excluded: one athlete could not perform a block start due to injury and the equipment failed during one run of another athlete. The trajectory data of the remaining runs was averaged and smoothed using Matlab. GCP-locations were measured as well. Initial contact angles and average minimum and maximum leg lengths were calculated from the trajectory data and GCP-locations. Physical constants such as mass, CoM height and prosthesis height were measured on site (see Table 3.2). A section of the plotted results is shown in Figure 3.6.

The smoothed velocity profile over the two runs is shown in Figure 3.7. The acceleration in the

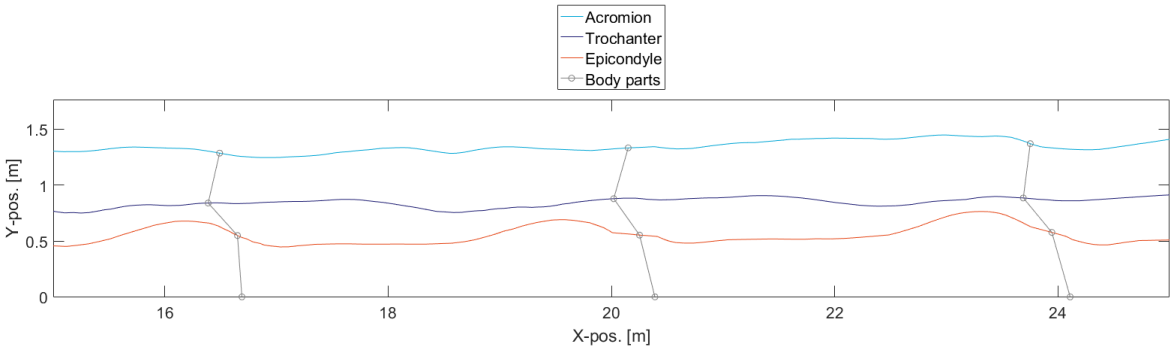

Figure 3.6: The plotted results of the motion analysis shows a section of the trajectories of the three bony landmarks that were tracked. The lower leg, upper leg and torso are plotted as line segments between the landmarks and the measured GCP. Note that only the trajectory of the affected leg is shown here.

Name	Symbol	Value
Mass	m	75 kg
CoM height	L_{cm}	1 m
Blade length	L_{s_0}	0.4 m
Max leg length	$L_{a_{max}}$	0.6 m
Min actuator length	$L_{a_{min}}$	0.45 m

Table 3.2: The physical constants of the subject were measured on site before the filming or calculated later from the trajectory data. These constants were later used in the simulation of the ASLIP model. See also Appendix B Table B.1

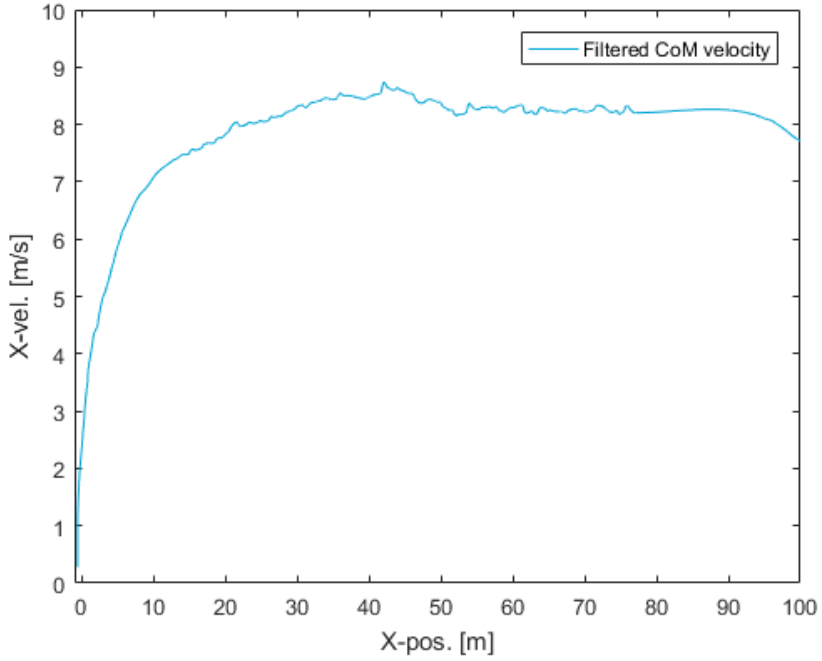

Figure 3.7: The filtered and smoothed velocity profile of the CoM of an unilateral transtibial amputee athlete during a 100m sprint.

first several meters is exceptionally high, even when compared to velocity profile of Usain Bolt (Figure 2.3). This acceleration is therefore unrealistic and probably the result of incorrect motion tracking due to lens distortion. Nonetheless, the shape of the velocity profile and the division between acceleration and steady state stage is recognisable and comparable to that of other athletes. Just as in able-bodied athletes, the CoM trajectory has a low vertical displacement; i.e. a 'smooth' ride. Spatiotemporal variables Lstep and Fstep are very similar to ABS: the athlete starts with a relatively high Fstep and a low Lstep. Both increase to their maximum values at top speed (see Figure 3.8).

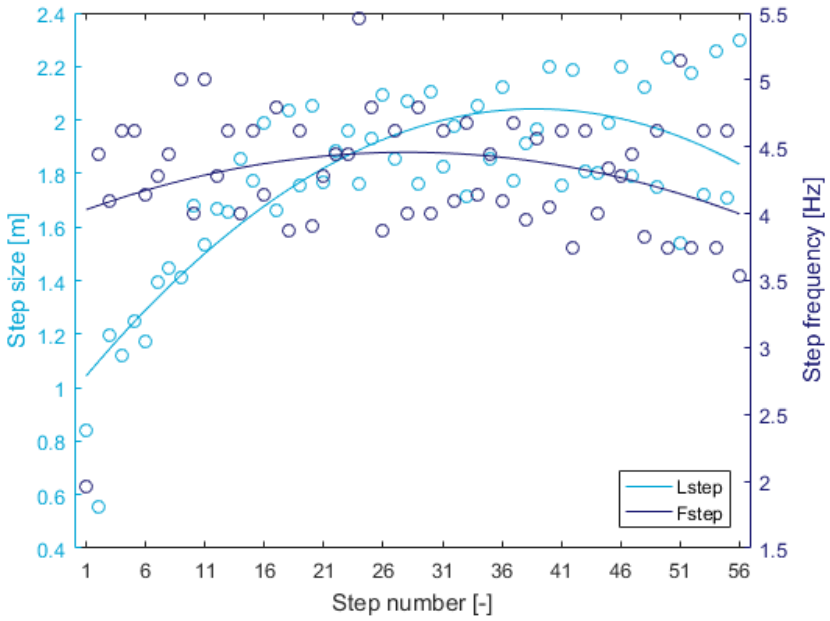

Figure 3.8: The measured step length and step frequency per step of an unilateral transtibial amputee athlete during a 100m sprint.

3.3. Actuated Spring-Loaded Inverted Pendulum

The motion data retrieved in the section provides starting point for the creation of a new model that is capable of simulating amputee sprinting. The proposed active dynamic model is based on the following assumptions about amputee sprinting:

1. Sprinting consists of two phases: acceleration and steady state.
2. The legs of amputee sprinters can be approximated by a mass on a massless linear spring.
3. Amputee sprinting motion can be described qualitatively by a simple active spring-mass system.
4. Performance gains for bilateral transtibial amputees also hold for other amputee sprinters.

It should be stressed that any additions to the model infringe on its simplicity and therefore its usefulness. More complex is not always better. As Blickhan put it himself: "The fact that the spring-mass model is successful in predicting and describing the general features of animal locomotion does not depend on a detailed agreement of the real leg with the assumed linear, massless spring." [7]. Complexity can hamper the use of numerical optimisation and stability might become a problem. More importantly, the more extensive a model becomes the harder it is to verify its results. Any addition to the model needs to be validated before it can be used, it is therefore advisable to keep these additions as simple as possible.

Relatively simple additions to SLIP model can make it suitable for simulating prosthetic sprinting specifically. It is apparent that energy should be added to the passive elastic spring-mass system to make it capable of describing motion during start and acceleration. Multiple options can provide this energy. For example, two springs in series with a mass in between or a 'knee' joint with a torque applied

to it. However, these additions would mean either adding inertia or extra independent parameters to the model and will therefore infringe on the model's simplicity. Instead, building on Blickhan's SLIP model, it was decided to add a separate set of motion equations that described the motion of the CoM under a constant force produced by a linear actuator. The actuator has a maximum stroke; it can accelerate the CoM until its length runs out. No extra joints or masses are added to the system in this way. In this simplest form of an Actuated Spring-Loaded Inverted Pendulum (ASLIP) model not two, but three sets of motion equations alternate. Furthermore, aerodynamic drag is introduced in the form of a velocity dependent force in the negative x-direction.

The ASLIP model consists of a sequence of three sets of motion equations:

Active contact phase (CA):

$$\ddot{x} = \frac{F_a}{m}\cos(\gamma) - \frac{F_d}{m} \tag{3.7}$$

$$\ddot{y} = \frac{F_a}{m}\sin(\gamma) - g \tag{3.8}$$

Passive contact phase (CP):

$$\ddot{x} = \frac{k}{m}(l_0 - l_s)\cos(\alpha) - \frac{F_d}{m} \tag{3.9}$$

$$\ddot{y} = \frac{k}{m}(l_0 - l_s)\sin(\alpha) - g \tag{3.10}$$

Aerial phase (A):

$$\ddot{x} = -\frac{F_d}{m} \tag{3.11}$$

$$\ddot{y} = -g \tag{3.12}$$

with

$$F_d = \frac{1}{2}\rho\dot{x}^2 C_d A \tag{3.13}$$

and variables x, y, m, α, k, l_s, l_0 and g as in Equations 3.1-3.4 from Section 3.1. Aerodynamic drag is introduced as an velocity dependent force F_d. The actuator force F_a acts on the body under force angle γ. Both the actuator force and the force angle are known a priori and are step specific, but assumed constant over each individual step cycle. Just as in the SLIP model, the instantaneous angle at initial contact α_i is also known beforehand, but it is not the same for all steps. The configuration of the model at any point is described by the coordinates of the CoM x, y and leg angle α. The gravitational force field g is the directed in the negative y-direction.

The solver loops through the motion equations as follows: CA → CP → A → CP. The switch from active contact to passive contact is made when maximum actuator length $L_{a_{max}}$ is reached. From passive contact to aerial and from aerial to passive contact is identical as in the SLIP model (see Section 3.1.1 and Figure 3.3). Switching from passive to active contact signifies the beginning of a new step cycle and is done when the spring has reached its maximum compression: i.e. when the y-component of the CoM velocity switches sign. Accordingly, the passive contact phase consists of two parts: first compression where energy is stored and secondly, after actuation, extension of the spring and release of energy to the system. A schematic overview of the sequence of motion equations is shown in Figure 3.9. Similarly to the SLIP model it is assumed that there are no viscous losses at heel-strike. The model has some physical constants that are known a priori and do not change over the race, those will be called 'constants'. Some of the model inputs are also known beforehand but can change per step or per couple of steps, they will be called 'variables'. The initial conditions are only given when the simulation is started. All other parameters discussed in further sections are outputs of the model. The parameters that make up the constants, step variable inputs and initial conditions are shown below.

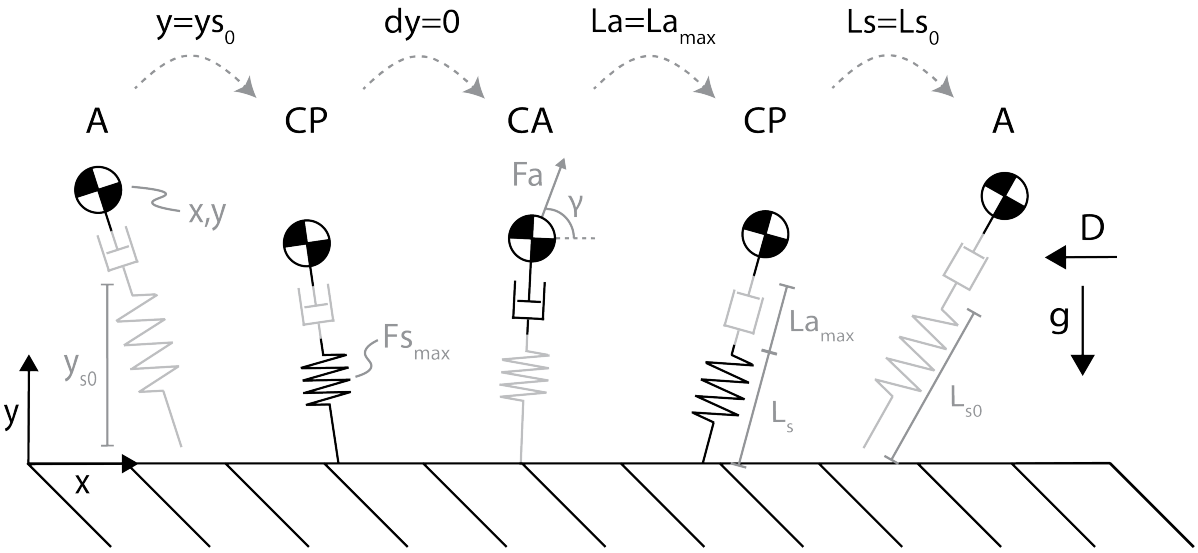

Figure 3.9: A schematic overview of the operation of the ASLIP model: the solver switches between motion equations when certain conditions are met (see also Equations 3.7-3.12).

Constants : $m, g, l_{s0}, l_{amin}, l_{amax}, C_d, \rho, A$
Variables : k, F_a, γ, α_i
Initial conditions : $x_0, y_0, x_{GCP0}, \dot{x}_0, \dot{y}_0$

3.3.1. Analysis of the ASLIP Model

The ASLIP model is solved in the same way as was explained in Section 3.1.1 (see Appendix C). The aerodynamic drag is calculated with constant air density $\rho = 1.225\ kgm^{-3}$ and a typical drag coefficient and frontal area of $C_d = 1$ and $A = 0.65\ m^2$. The other physical constants and input variables were retrieved from the motion analysis (see Table 3.2). Actuator force is assumed to lie around $F_a \approx 1.5\ BW$, which is an estimate of the mean stance averaged force produced during sprint running [1]. Force angle varies per step but is taken between 80 and 90 degrees: $80° < \gamma < 90°$ [32], with a general trend of more forwardly oriented during start and acceleration ($\gamma = 80°$) and more vertically ($\gamma = 90°$) towards the end of the race [36]. This is similar to what can be seen on the images of the amputee sprinter in Section 3.2. To achieve stability as well as a motion pattern similar to the actual trajectory, the actuator force and force angle were fine-tuned within these limits. In practice this meant that the first steps of the model required a higher actuator force and a sharper force angle. Although this was not measured, it is not unlikely to be the case in practice as well: during acceleration the athlete leans more forward and is still able to produce maximum power. The touchdown angle was retrieved from the motion analysis: $100° < \gamma < 120°$. The actuator force F_a, force angle γ and touchdown angle α_i per step can be found in Appendix B Table B.1. Stiffness was taken constant at $k = 3\ kNm^{-1}$. With these parameters the model settles into a stable stride pattern. The simulated CoM motion for three steps is plotted in Figure 3.10.

For equal physiological constants, the motion described by the model at any stage in the race is very similar to what is seen in actuality. The motion of the ASLIP model is sinusoidal with low vertical displacement. Although the tracked CoM trajectory cannot be fitted with a sinusoid, it is an oscillating motion and shows similar displacement (see Figure 3.11). More importantly, the GCP positions match closely to those of the model (mean absolute horizontal position error = 19 cm) even though this position is not imposed on the model; it is a result of the simulation parameters. As can be seen in Figure 3.12, the horizontal velocity of the ASLIP CoM matches the filmed data well, except for the acceleration stage. However, as was discussed earlier, the validity of this part of the filmed data is questionable. The initial acceleration of the ASLIP model is actually believed to be more realistic. The mean finishing time of the filmed athlete was 14.29 s, the ASLIP model finished in 14.65 s.
The spatiotemporal output of the model matches that of the amputee sprinter (Figure 3.13). Step

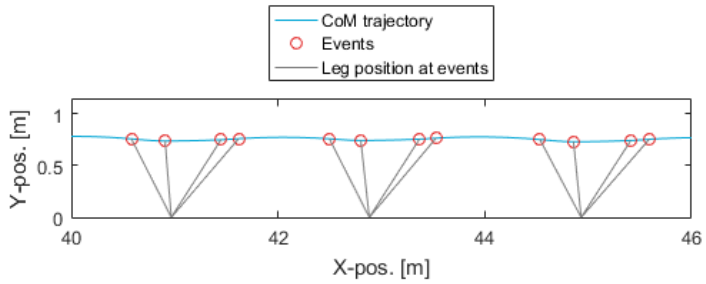

Figure 3.10: The CoM trajectory of the ASLIP model plotted together with the leg positions at the 'events'. The events in the simulation signify when the solver switches from equations of motion. The sequency of motion equations can be found in Section 3.3.

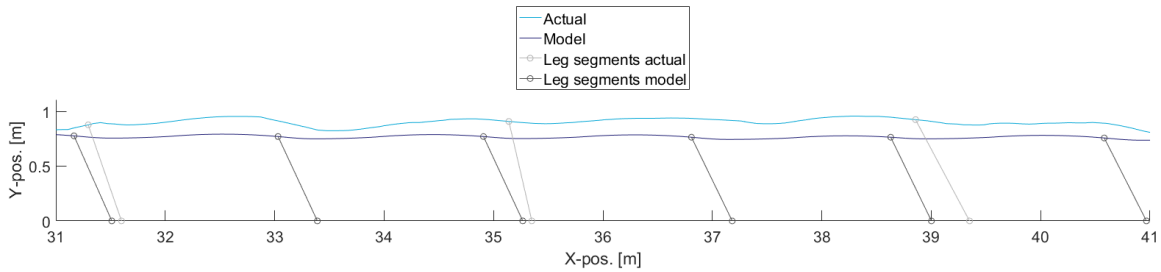

Figure 3.11: The CoM trajectory of the amputee sprinter and the CoM motion of the ASLIP model plotted together with their respective leg positions at inital contact. Note that for the amputee sprinter only the affected leg was tracked and plotted.

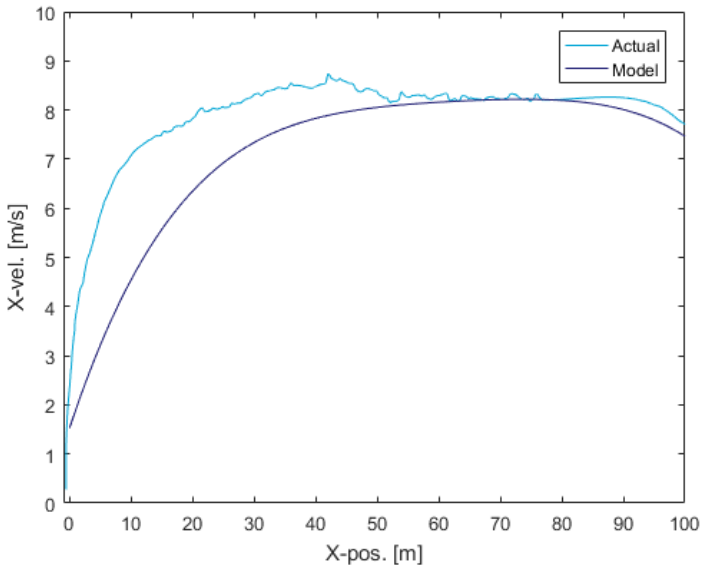

Figure 3.12: The horizontal velocity of the amputee sprinter versus that of the ASLIP model. The actual initial acceleration is much higher, but it is assumed that this is due to a tracking error made during the motion analysis.

size and step frequency are generally similar. With these simulation parameters the model is not able to achieve a similar step frequency in the first part of the 100m (Figure 3.13b). This is due to the combination of actuator force F_a and force angle γ applied here. Both parameters have a large influence on the step frequency which in turn has a strong interdependency with step size. The trial-and-error approach of tuning these parameters used in this section proved to be inefficient. The step frequency discrepancy will be solved in Chapter 4 using a different approach.

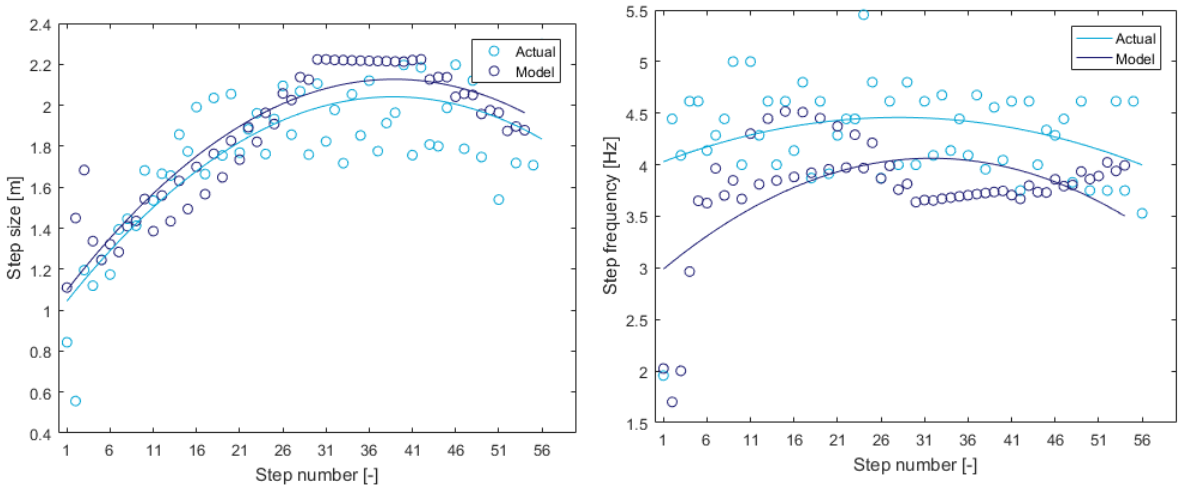

(a) The step size of the amputee sprinter versus that of the ASLIP model.

(b) The step frequency of the amputee sprinter versus that of the ASLIP model.

Figure 3.13: The step size and frequency of the amputee sprinter versus those of the ASLIP model.

The ASLIP model describes amputee sprinting well. The output of the model describes the same smooth running pattern as is observed in human running [2, 31]. The velocity profile of the spring-mass model closely resembles that of the filmed amputee sprinter. Just as the SLIP model, the ASLIP is not a quantitative description of amputee sprinting. Simulation parameters such as actuator force Fa and force angle γ are taken close to leg forces and force angles reported in literature, but are not physically correct. Nonetheless, the qualitative output of the model, i.e. the model behaviour, is very similar to that of actual amputee sprinters and it can therefore be concluded that the model is accurate enough to be used as a description of amputee sprinting.

4

Optimal Sprinting Performance

Optimal performance of the ASLIP model depends largely on the combination of step-specific input parameters. The ASLIP model is a qualitative description of amputee sprinting. In contrast to the initial conditions and physiological constants, these parameters may therefore take values deviating from what is reported in literature as long as the described motion is physiologically achievable (see Chapter 3 Section 3.2). In other words, there might exists a range of possible combinations that lead to different but still feasible model output. This implies that the optimal combination is not easily found with a trial-and-error method. Not in the least place because small deviations in the input of the model can lead to instability and therefore no performance at all. In this section an attempt is made to find such a combination using numerical optimisation methods.

4.1. The Effect of Stiffness on Sprinting Performance

Firstly, the sensitivity of the validated ASLIP model to change in stiffness is tested. Recall that it was hypothesised that amputee sprinting performance would increase with a stiffer prostheses at the start of the race. With a higher spring stiffness it is expected that the model will accelerate faster (see Section 2.2). To test this hypothesis the ASLIP model is simulated with a range of physiological acceptable RSP stiffness. All other parameters were kept constant. The results are plotted in Figure 4.1.

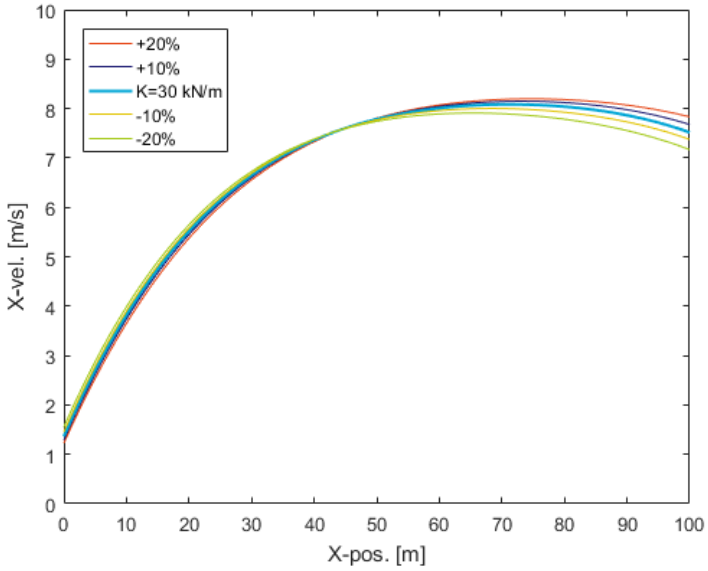

Figure 4.1: The effect of different spring stiffness on the horizontal velocity profile of the ASLIP model. All other simulation parameters are kept constant.

In the model, increase of spring stiffness leads to higher top speed but not faster acceleration. On

the contrary, acceleration is slightly impaired. This might be the result of the structure of the model: the events that signify the switch between the motion equations partly determine the effect of the simulation parameters on the output. In particular the switches between phases CP and CA (see Section 3.3) are important regarding the effect of stiffness on the overall performance of the model.

Two additional scenarios were tested to check the relevancy of the event functions on the model output. The reference scenario (scenario 1) is as proposed in Section 3.3. Scenario 2 switches from CP to CA when the force in the spring equals the actuator force $Fs = Fa$. F_a is a constant pre-imposed force. Scenario 3 switches from CP to CA when the force in the spring switches sign (identical to scene 1), but instead the actuator force is not constant but equals the max force in the spring $F_a = F_{s_{max}}$. However, these scenarios led to similar results or unrealistic CoM motion (scenario 3).

The ASLIP model does not confirm the hypothesis that higher spring stiffness lead to faster acceleration. Nonetheless, it seems that a stiffer spring does prolong the acceleration phase: steady state is reached later and top speed is higher. In this sense, sprinting performance is better with a higher spring stiffness. For example, the finishing time of the ASLIP model for k=30 kNm^{-1} is 14.65 s, for a 20% higher stiffness k=36 kNm^{-1} it is 14.62 s. This might seem like a marginal gain, but it can make the difference in a 100m sprint. Moreover, only a constant spring stiffness is tested in this section. The effect of phase specific spring stiffness is unknown. Consequently, this can be seen as an indication that performance gain is possible here. In addition, the model output strongly depends on the specific combination of simulation parameters (e.g. F_a, γ, α_i and k) and the influence of these combinations should therefore be tested. Optimisations algorithms that are explained in the next section are capable of efficiently doing so.

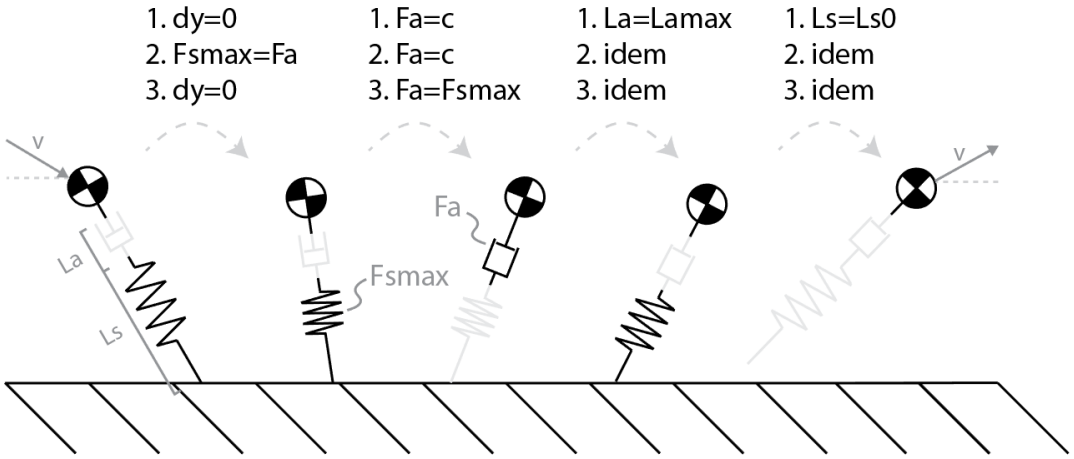

Figure 4.2: Three different scenarios with corresponding events that signify a switch between the phases CP and CA (see Section 3.3).

4.2. Optimisation of the ASLIP Model

Optimal performance in amputee sprinting is considered to be equivalent to minimal time to completion of the 100m sprint. The goal of the optimisation of the ASLIP model is therefore to minimise finishing time T_{fin}, which is a function of the step dependent optimisation variables $k(s)$ $[kNm^{-1}]$ & $\alpha_i(s)$ [°], the simulation parameters $F_a(s)$ $[BW]$ and $\gamma(s)$ [°] and the physical constants Pc (see Table 3.2). The optimisation problem in its most general form can be stated as follows:

$$\min_{k(s),\alpha_i(s)} \; T_{fin}(k(s), \alpha_i(s), \gamma(s), F_a(s), Pc)$$
$$\text{s.t. } 24 \leq k \leq 36$$
$$96 \leq \alpha_i \leq 126$$

where the upper and lower bounds result from the optimality criteria $k_{opt} = K_0 \pm 20\%$ & $\alpha_{i_{opt}} = \alpha_{i_0} \pm 5\%$. These criteria are based on experience with the ASLIP model (Section 3.3.1) and literature. No further constraints or (in)equalities exist. If for a certain set of variables the system becomes unstable

and is not able to complete the 100m, the simulation breaks and the solver will try a different step. As a default the pattern search algorithm of Matlab is used. This is a type of grid search that is likely to find a global optimum.

4.2.1. Phase-Specific Stiffness

The optimisation problem is solved to find optimal phase-specific stiffness (see Appendix C). All other parameters are fixed and remain unchanged from the values found in Chapter 3 Section 3.3.1. For an overview of the step-specific parameters please see Appendix B Table B.1. As an initial guess, the same constant spring stiffness as before is taken $k = 30\ kNm^{-1}$. In order to keep computation time within reasonable limits the stiffness is changed only every 10 steps:

$$K_0 = \begin{bmatrix} 30 & 30 & 30 & 30 & 30 & 30 \end{bmatrix}$$

With these parameters the solver finds an optimum phase-specific stiffness of:

$$K_{r\,opt} = \begin{bmatrix} 35.1 & 35.6 & 35.6 & 34.7 & 34.1 & - \end{bmatrix}$$

which will be called the reference stiffness from here on. The model finishes in 14.55 s with a physiologically feasible gait similar to that reported in the previous chapter. The other outputs of the optimisations are plotted in Figure 4.3 and Figure 4.4 Step frequency and step length fall within a physiologically reasonable range.

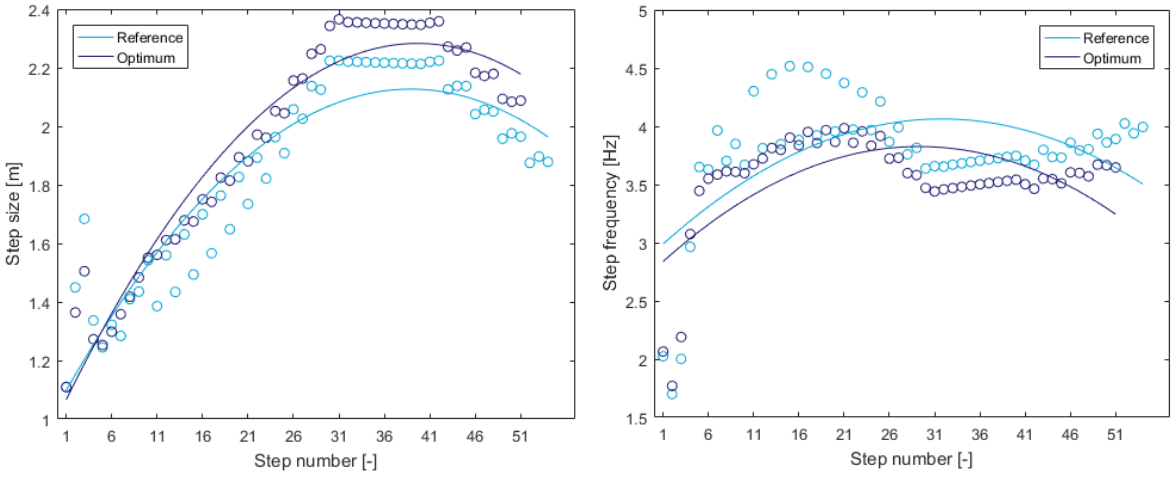

(a) The step size for optimal phase-specific stiffness versus the constant stiffness.

(b) The step frequency for optimal phase-specific stiffness versus the constant stiffness.

Figure 4.3: The step size and frequency corresponding to the calculated optimal phase-specific stiffness versus the constant stiffness.

Phase-specific stiffness leads to a significant performance benefit in the ASLIP model of amputee sprinters. The found optimum is 0.1 s faster than constant stiffness. In comparison: when the solver is ran for a single constant stiffness it results in maximum allowed stiffness ($K = 36\ kNm^{-1}$) and an only slight reduction in finish time ($T_{fin} = 14.62\ s$). The velocity profile shows that the model is able to prolong the acceleration stage, reaching a higher top speed. This can be explained by the fact that a stiffer spring reaches its full compression faster, therefore starting actuation earlier in the contact phase. Consequently, the energy stored in the spring is utilised but released more vertically. This results in a bigger step size and a lower step frequency (see Figure 4.3). At slower speeds this effect is less pronounced as the energy stored in the spring is lower and therefore relatively less important to the overall energetics. The acceleration penalty for increased constant stiffness that was seen in Section 4.1 is not as significant for this phase-specific stiffness. The model with phase-specific stiffness does indeed seem to be able to achieve similar step size and frequency during start and acceleration. Furthermore, it seems that the higher velocity in the latter part of the race is achieved by increasing step size (Figure 4.3a) rather than step frequency. Other simulation parameters that are kept fixed might play a role here.

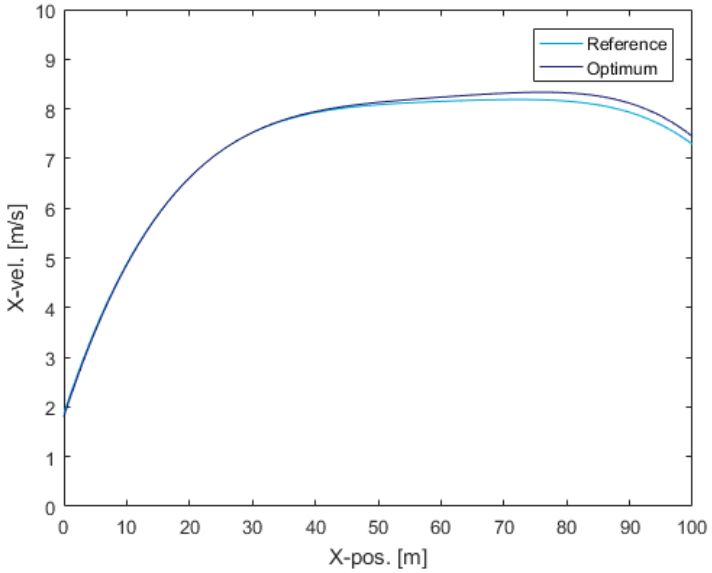

Figure 4.4: The horizontal velocity profile corresponding to the optimal phase-specific stiffness versus that of the constant stiffness.

Phase-specific stiffness is strongly influenced by the simulation parameters (e.g. F_a, γ, α_i and k). It seems that the found optimal stiffness in this section is related to velocity and actuator force. For the first 10 steps the horizontal and vertical velocity of the CoM are low. The model benefits from a slightly softer spring. The optimal stiffness for the next 10 steps than increases with speed. That this increase does not progress from step 20 to 30 might be explained by the fact that the actuator force goes down from $F_a = 1.7\ BW$ to $F_a = 1.5\ BW$ (see also Figure 4.5). This counterbalances the velocity increase that is observed over those steps. In addition, the optimal stiffness of $35.6\ kNm^{-1}$ is already close to the upper bound. The acceleration phase ends around 40 m into the race at step no. 26. This explains the sharp decline in optimal stiffness for the last 20 steps. Furthermore, touchdown angles at this point are at its highest (120°) and remain that way until the very last part of the race.

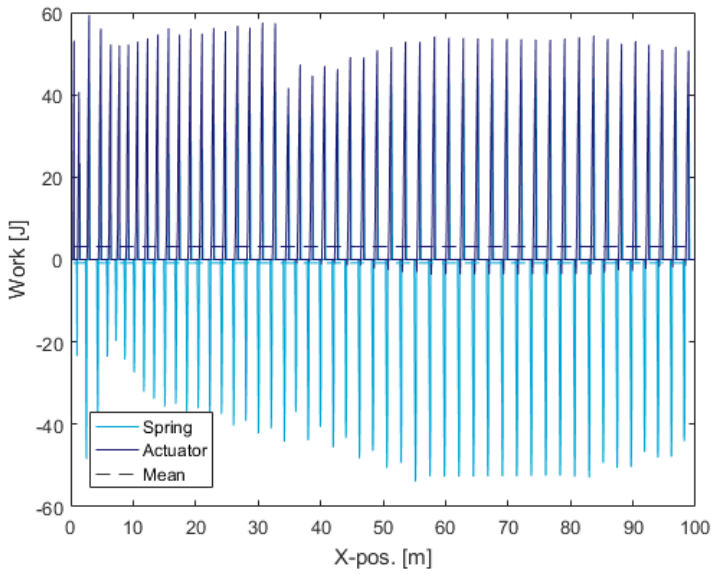

Figure 4.5: The work done by the spring and actuator of the ASLIP model for the optimal phase-specific stiffness.

4.2.2. Interdependency of Parameters

The interdependency of these parameters can be investigated by increasing the parameter space of the optimisation problem. Because the aim of this study is to investigate the effect of stiffness on sprinting performance, care must be taken to what parameters are added to the optimisation. For example, optimising for actuator force F_a results in forces close to the upper boundaries imposed on the system and unreasonably high step sizes. Naturally, more energy in the system will lead to better performance. However, the part of this performance benefit that can be attributed to the stiffness is unclear. In other words, the output of the optimisation should not only be physiologically feasible but it must be possible to extract the effect of stiffness on the performance. Because force F_a and force angle γ both directly influence the amount of propulsive force that is applied to the CoM it is decided to keep them outside of the optimisation. Touchdown angle α_i does not directly influence the energetics of the system. Instead it acts on the timing of the passive and elastic phases of the model. It might therefore be an enabler for performance. This section investigates the effect of the free variables stiffness k and touchdown angle α_i on the model performance.

The optimisation problem is solved with free variables stiffness and touchdown angle. All other parameters and constraints are unchanged from previous sections. To reduce computational time the touchdown angle is changed only every other step. As an initial guess, similar values in Section 3.1.1 are used (see Table B.2). The initial guess for stiffness (every 10 steps) is taken $k = 30\ kNm^{-1}$. With these parameters the solver finds an optimum phase-specific stiffness of:

$$K_{opt} = \begin{bmatrix} 24.8 & 35.9 & 33.8 & 32.8 & 35.8 & 33.2 \end{bmatrix}$$

and the model finishes in 14.38 s. Optimal touchdown angles are plotted in Figure 4.6. The model settles in a stable gait, but the feasibility of the motion pattern is questionable. Figure 4.7 shows part of the CoM trajectory. The model has an asymmetrical gait pattern that is uncommon for sprinters. The step size and step frequency for some steps go beyond what is considered to be achievable for amputee athletes during a 100m sprint (Figure 4.8). A 'skipping' gait as shown in Figure 4.7 seems to be a reaction to an abrupt reduction in actuator force. It often starts at the first step right after the force is lowered (step 21). An oscillation in CoM velocity -in particular vertically- and model energetics -in particular work done by the spring- is noticed during this part of the race as well. It seems that the model responds in an under-damped way to the new energy equilibrium.

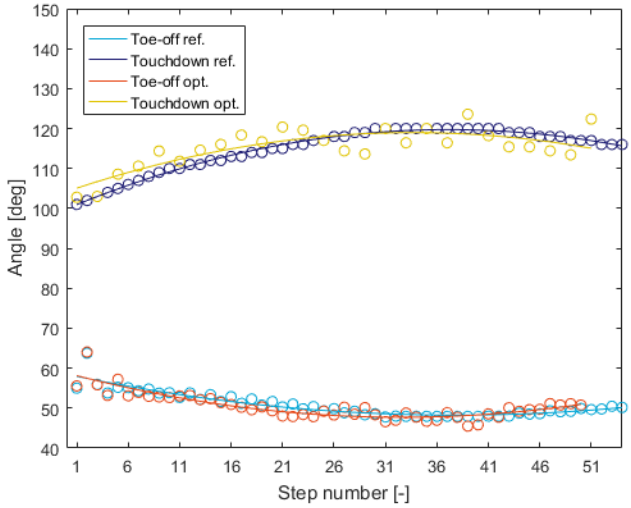

Figure 4.6: The optimised touchdown and resulting toe-off angles for corresponding optimal stiffness.

Optimisation of both spring stiffness and touchdown angle results in better performance, but does not yield physiological feasible results. Extending the boundaries for the optimisation variables does not solve this problem. The optimisation is not correctly constrained to be used to investigate the effect of this increased parameter space. Nonetheless, it can be concluded that optimal stiffness is influenced by touchdown angle. Namely, the optimal stiffness depends on the timing of compression

and extension of the spring. As can be seen in Figure 4.6, touchdown and toe-off angles are strongly correlated. In the model, these angles govern the timing of energy storage and release because they determine when the model switches to and from the passive motion equations. Indeed, by optimising the touchdown angle the model was -although unrealistically- enabled to increase step frequency. This indicates that variable spring stiffness most probably requires a gait change as well. To what extend this is possible in actuality can only be found out with physical experiments.

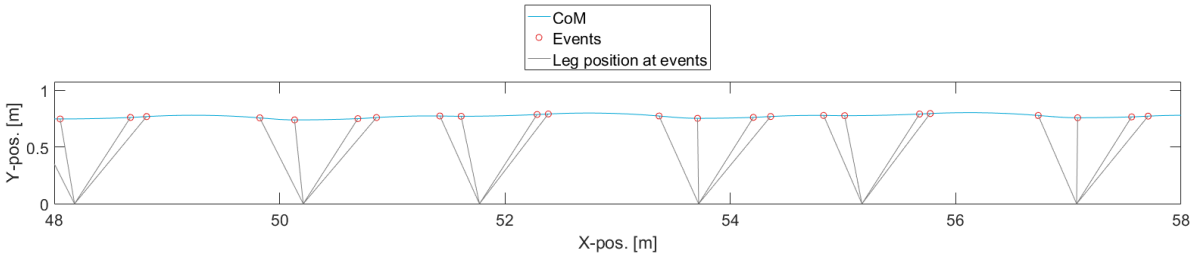

Figure 4.7: The CoM trajectory of the ASLIP model for optimised variables stiffness and touchdown angle plotted together with the leg positions at the events.

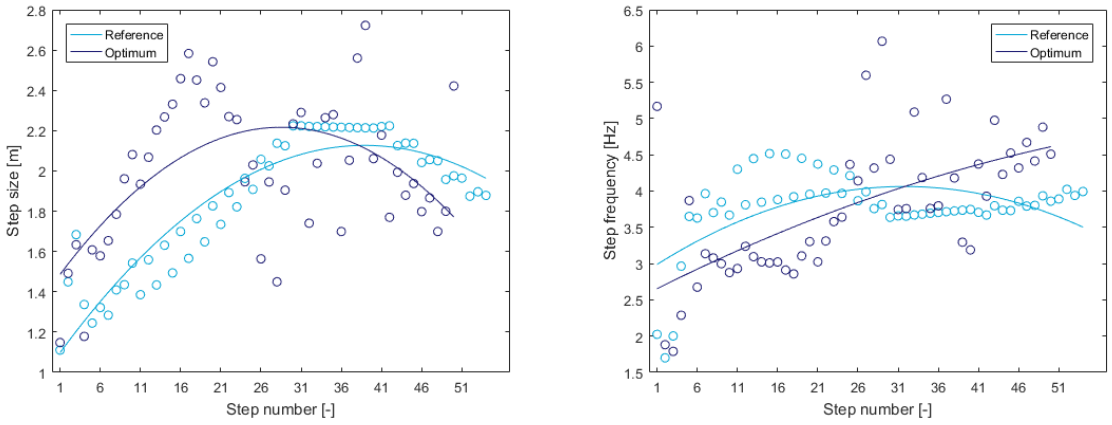

(a) The step size of optimal versus reference stiffness and touchdown angle.

(b) The step frequency of optimal versus reference stiffness and touchdown angle.

Figure 4.8: The spatiotemporal parameters corresponding to the optimised variables stiffness and touchdown angle versus the parameters corresponding to the constant reference values.

4.3. Sensitivity Analysis

The previous section shows that the model output is sensitive to the combination of its inputs. In order to identify to what extend the found phase-specific stiffness is responsible for performance, this section focusses on the accuracy and sensitivity of the optimisation. No solver in Matlab is able to find a true global minimum, but it is possible to test the sensitivity of the solver to local minima by testing multiple initial points. Three different initial guesses are investigated. K_{1_0} and K_{2_0} are on the extremes of the imposed boundaries and K_{3_0} is the inverse of the hypothesised outcome. All other parameters and constraints are unchanged.

$$K_{1_0} = \begin{bmatrix} 25 & 25 & 25 & 25 & 25 & 25 \end{bmatrix}$$
$$K_{2_0} = \begin{bmatrix} 35 & 35 & 35 & 35 & 35 & 35 \end{bmatrix}$$
$$K_{3_0} = \begin{bmatrix} 26 & 28 & 30 & 32 & 34 & 36 \end{bmatrix}$$

For these initial guesses the solver finds optima as follows:

$$K_{1_{opt}} = [30.0 \quad 29.1 \quad 27.6 \quad 29.6 \quad 29.1 \quad 29.6]$$
$$K_{2_{opt}} = [34.7 \quad 35.0 \quad 26.6 \quad 35.5 \quad 35.5 \quad 30.9]$$
$$K_{3_{opt}} = [35.1 \quad 35.9 \quad 35.2 \quad 34.1 \quad 34.0 \quad 34.0]$$

$$K_{r_{opt}} = [35.1 \quad 35.6 \quad 35.6 \quad 34.7 \quad 34.1 \quad -]$$

These optima produce similar gaits and performance ($T_{1_{fin}} = 14.64\ s$, $T_{2_{fin}} = 14.52\ s$ & $T_{3_{fin}} = 14.54\ s$) as the reference case from Section 4.2.1 ($T_{r_{fin}} = 14.54\ s$). Furthermore, the stiffness shows the same general trend as in other optimisations.

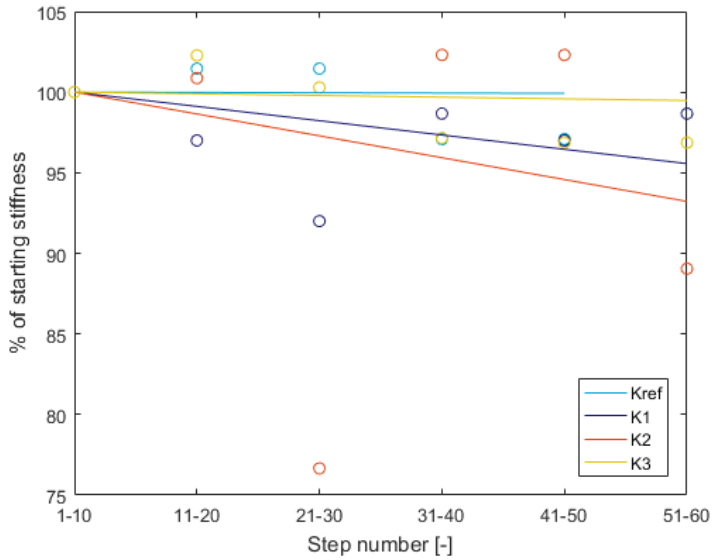

Figure 4.9: The found optimal phase-specific stiffness for different optimisation initial points. The found values are shown relative to the stiffness at start.

In addition, small deviations around the found optimum reference stiffness $K_{r_{opt}}$ from Section 4.2.1 are tested. Increasing the stiffness with small percentages for all phases leads to marginal performance gains. The inverse happens for decreasing the stiffness. Skewing the phase-specific stiffness to completely regressive or progressive does not seem to significantly influence performance.

Step no.:	**1-10**	**11-20**	**21-30**	**31-40**	**41-50**	**51-60**	T_{fin} [s]	T_{fin} %
$K_{r_{opt}}$: [kNm^{-1}]	35.1	35.6	35.6	34.7	34.1	34.1[1]	14.55	-
K_{test} :	-10%	-10%	-10%	-10%	-10%	-10%	14.62	+0.44%
	-5%	-5%	-5%	-5%	-5%	-5%	14.58	+0.22%
	+5%	+5%	+5%	+5%	+5%	+5%	14.52	-0.25%
	+10%	+10%	+10%	+10%	+10%	+10%	14.50	-0.36%
	-10%	-10%	-10%	+10%	+10%	+10%	14.57	+0.11%
	-5%	-5%	-5%	+5%	+5%	+5%	14.55	+0.01%
	+5%	+5%	+5%	-5%	-5%	-5%	14.54	-0.07%
	+10%	+10%	+10%	-10%	-10%	-10%	14.54	-0.08%

Table 4.1: The sensitivity of the performance of the ASLIP model to small deviations in the phase-specific stiffness.

Sprinting performance of the ASLIP model is not strongly influenced by change in spring stiffness only. It does seem that in general the model is performing better with a globally regressive phase-specific stiffness. Furthermore, a stiffer spring performs better than a compliant one. The optimisation is sensitive to local minima. However, a slight regressive stiffness trend can be observed for all optima. It must be noted that this analysis is performed while all other parameters are kept fixed. The found optimal stiffnesses did indeed not lead to significant changes in gait pattern. They are therefore to be seen as optima that hold only for the contact angles that are imposed on this model.

[1] The model finishes in 50 steps with the optimal reference stiffness. Because it is required to define an initial stiffness guess for at least 60 steps, the remaining 10 steps are taken equal to the preceding 10 steps.

5

Discussion

The Actuated Spring-Loaded Inverted Pendulum (ASLIP) model proposed in this research is capable of qualitatively describing amputee sprinting motion. The work done shows that a simple active spring-mass model can predict the CoM motion and gait pattern of amputee sprinters accurately and effectively. The model is remarkably stable and has the key characteristics of human sprinting, namely: low vertical CoM displacement [7], low touchdown angles [33] and step sizes and frequencies inside the physiologically feasible range of $1.7\ m \leq Lstep \leq 2.2\ m$ and $1.7\ Hz \leq Fstep \leq 2.2\ Hz$ respectively [15, 19]. The ASLIP model furthermore enabled the use of numerical optimisation methods to test the effect of prosthetic properties on sprinting performance. The simulations revealed that introducing phase-specific stiffness will lead to a reduction of finishing time of the model.

In general, the model performed better with a higher spring stiffness. With a phase-specific stiffness of every 10 steps the model is able to achieve even faster finishing times. Furthermore, it seemed that all of the found phase-specific optima have a similar stiffness trend: the stiffness is highest during initial acceleration and lowest towards the end of the race. Although these optima did not lead to faster acceleration, they did result in a higher top speed. The model seemed to be able to prolong acceleration with a higher spring stiffness. The simplicity of the spring-mass model additionally allowed for an investigation of parameter sensitivity and interdependency. This analysis showed that optimal phase-specific stiffness is most sensitive to input parameters such as the imposed touchdown angle and actuator force.

Recently, it has been suggested that the optimal stiffness is largely dependent on gait phase and amputee sprinting performance might be impaired by constant prosthetic stiffness [34]. In addition, it has been shown that in general athletes can benefit from a stiffer prosthesis at the start and a more compliant one towards the end of a race [13, 35]. The results of this research support these findings and augment them by showing that touchdown angle and force application are important determinants of optimal stiffness. However, despite that there is compelling evidence that higher stiffness will lead to faster acceleration [13, 23, 34], the model does not substantiate this. In fact, the model even predicts an slightly inverse relationship between stiffness and acceleration. It thus seems that the simple active spring-mass model does not completely explain the underlying mechanisms that cause amputee sprinting performance.

It must be stressed that the validity of the ASLIP model has its bounds. Firstly, the active spring-mass model is not a quantitative description of amputee sprinting. Although input parameters are taken within physiological limits [1, 32, 36], the model does not include detailed descriptions of leg segments or muscle dynamics and its results can therefore not be transferred to the physical world without critically reviewing them. Secondly, the ASLIP model is not actually an active bouncing system, but a concatenation of active and passive systems. In other words, the active and elastic elements of the ASLIP model never act together: there is no direct effect of the actuator on the spring or vice versa. This can explain the effect of phase-specific stiffness on acceleration and top speed. In addition, the model does not distinguish between leg and prosthetic stiffness. In actuality, the leg muscles are mechanically coupled to the prosthetic device and the total perceived stiffness is the combination of leg stiffness and mechanical prosthetic stiffness [24, 28, 37]. Nonetheless, the predictions made by the model do give an indication of where and how to gain sprinting performance and provides insight into

the relationships between relevant performance parameters.

The evidence presented indicates that amputee sprinting performance is not determined by a single parameter alone. The optimal stiffness depends on the combination of multiple gait phase dependent parameters, e.g. touchdown angle, muscle force, force angle and CoM velocity. Because these parameters change per gait phase [11] it is clear that the mechanical properties of prosthetic sprinting devices should too. Furthermore, it needs to be taken into account that a change in sprinting gait might be required in order to fully benefit from phase-specific spring stiffness. During acceleration, amputee athletes might be able to achieve even sharper touchdown angles with phase-specific stiffness, possible resulting in a smoother and faster ride with step frequencies higher than what is currently seen. Regardless, the introduction of phase-specific stiffness alone can already result in 0.1 $\pm$0.05s reduction of finishing time, which is a significant performance benefit in the 100m sprint. On its own, this is already a strong indication that more is to be gained in this direction. However, before Running-Specific Prostheses with phase-specific stiffness can be developed, more research is necessary to better understand the underlying mechanisms that determine amputee sprinting performance.

Two additions to the ASLIP model are recommended that could directly improve the accuracy of the predictions and provide further answers to the main question:

1. Implementing a mechanical coupling between the spring and actuator.
   Such a coupling would add independent parameters to the problem and would therefore increase the complexity of the model. However, this extension of the model could also provide a deeper insight on the effect of stiffness on sprinting performance.

2. Implementing constraints on spatiotemporal parameters.
   For this thesis the parameter space of the optimisation was kept small in order to achieve realistic outputs and reduce computational costs. With higher computing power combined with appropriate constraints that constrain spatiotemporal parameters such as step size, frequency and/or vertical displacement of the CoM to within physiological limits, it is possible to investigate the true potential of phase-specific stiffness.

The applicability of forward dynamic modelling does not stop with these additions alone. The simplicity and effectiveness of forward dynamic models such as the ASLIP model make them very well suited for sports engineering research. The modelling approach as a research and design tool is promising and much more versatile than presented in this thesis.

6

Conclusion

Gait phase-specific stiffness of sprinting prostheses leads to enhanced performance in a forward dynamic model of amputee sprinting. The simple active spring-mass model proposed in this thesis is successful in describing the general features of amputee sprinting. This implies that amputee sprinting motion can be approximated by an active bouncing system. The model predicts a significant reduction in finishing time for a gait phase-specific spring stiffness in comparison to a constant stiffness. Generally, the optimal phase-stiffness is higher during start and acceleration as compared to steady state. However, this is not due to faster acceleration, but a higher top speed. Although these predictions made by the model should not be blindly taken over by prosthetic manufactures, they do give an indication of the direction for further research. The evidence presented in this thesis suggest that amputee athletes might be able to reduce their sprinting times with prosthetic devices with a regressive phase-specific stiffness. Above all, this thesis proves that acceleration and steady state phases of the 100m sprint require a different prosthetic stiffness. It is very well possible that in the future prosthetic sprinting devices with phase-specific stiffness become the new standard, perhaps even inducing a similar spike in performance as was observed after the introduction of carbon running-specific prostheses.

A

Camera Setup

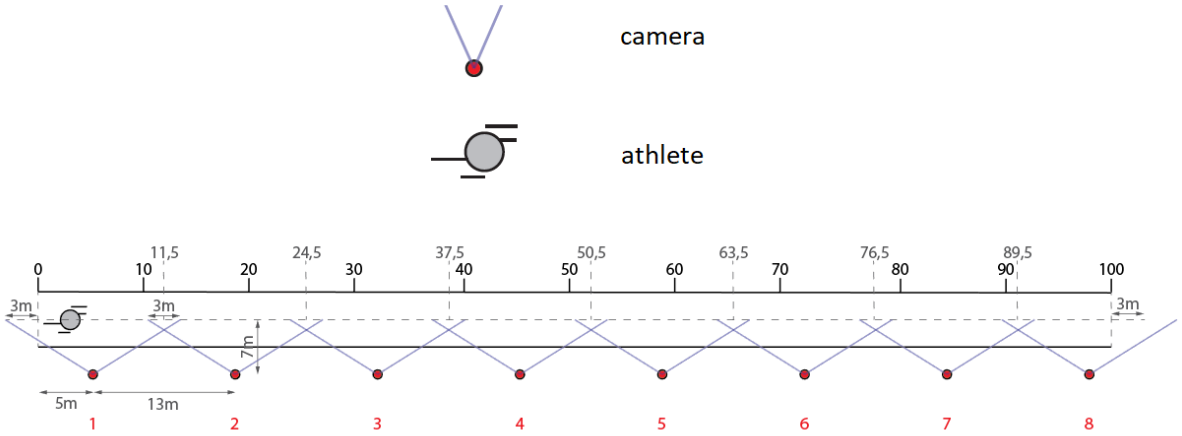

Figure A.1: A schematic top view of the camera setup used during the filming of the 100m sprint of three amputee athletes at Papendal. The motion was captured from the side.

B

Simulation Parameters

Step no.	$Fa\ [BW]$	$\gamma\ [\circ]$	$\alpha_i\ [\circ]$	**Step no.**	$Fa\ [BW]$	$\gamma\ [\circ]$	$\alpha_i\ [\circ]$	**Step no.**	$Fa\ [BW]$	$\gamma\ [\circ]$	$\alpha_i\ [\circ]$
1	2	60	101	**21**	1.5	80	115	**41**	1.5	90	120
2	1.7	70	102	**22**	1.5	80	116	**42**	1.5	90	120
3	1.7	75	103	**23**	1.5	80	116	**43**	1.5	90	119
4	1.7	80	104	**24**	1.5	80	117	**44**	1.5	90	119
5	1.7	80	105	**25**	1.5	80	117	**45**	1.5	90	119
6	1.7	80	106	**26**	1.5	85	118	**46**	1.5	90	118
7	1.7	80	107	**27**	1.5	85	118	**47**	1.5	90	118
8	1.7	80	108	**28**	1.5	85	119	**48**	1.5	90	118
9	1.7	80	109	**29**	1.5	85	119	**49**	1.5	90	117
10	1.7	80	110	**30**	1.5	85	120	**50**	1.5	90	117
11	1.7	80	110	**31**	1.5	85	120	**51**	1.5	90	117
12	1.7	80	111	**32**	1.5	85	120	**52**	1.5	90	116
13	1.7	80	111	**33**	1.5	85	120	**53**	1.5	90	116
14	1.7	80	112	**34**	1.5	85	120	**54**	1.5	90	116
15	1.7	80	112	**35**	1.5	85	120	**55**	1.5	90	115
16	1.7	80	113	**36**	1.5	85	120	**56**	1.5	90	115
17	1.7	80	113	**37**	1.5	85	120	**57**	1.5	90	114
18	1.7	80	114	**38**	1.5	85	120	**58**	1.5	90	114
19	1.7	80	114	**39**	1.5	85	120	**59**	1.5	90	113
20	1.7	80	115	**40**	1.5	85	120	**60**	1.5	90	113

Table B.1: The step dependent simulation parameters used to validate the proposed ASLIP model. Angle α_i was measured in the motion analysis. Force Fa and force angle γ were taken close common values reported in literature [1, 32] and fine-tuned in order to achieve a stability and motion comparable to the filmed data (see Chapter 3).

Step no.	α_{i0} [◦]	**Step no.**	α_{i0} [◦]	**Step no.**	α_{i0} [◦]
1-2	101	**21-22**	115	**41-42**	120
3-4	103	**23-24**	116	**43-44**	119
5-6	105	**25-26**	117	**45-46**	119
7-8	107	**27-28**	118	**47-48**	118
9-10	109	**29-30**	119	**49-50**	117
11-12	110	**31-32**	120	**51-52**	117
13-14	111	**33-34**	120	**53-54**	116
15-16	112	**35-36**	120	**55-56**	115
17-18	113	**37-38**	120	**57-58**	114
19-20	114	**39-40**	120	**59-60**	113

Table B.2: The initial contact angles that were taken as initial guess for the optimisation problem of Section 4.2.2. Other parameters as reported in Table B.1 above.

C

Matlab Code

The fundamental scripts that are used for this thesis can be found below. The author can be asked for the complete set of scripts.

C.1. SLIP Model

```
% Govert van der Gun, #4512235
% RUNME PASSIVE SLIP - 2DOF - ODE

clc
clearvars
close all

% constant properties of the body, spring and actuator
m=64; % mass of body in [kg]
g=9.81; % gravitational force field [N/kg]
ls0=0.9; % resting spring length [m] (measured from Levi = 0.4m)
k=2; k=k*10000; % stiffness in [N/m]

% initial contact angels [deg]
ain=repmat(25,60,1)+90;

ain=ain.*pi/180;
%% Pre-processing
% Running time
t0=0; % start time [s]
tend=40; % maximum time to simulate [s]
xend=100; % maximum distance to simulate in [m]
steps=60; % maximum number of steps to simulate [-]

% Initial conditions
a0=ain(1); % inital leg angle [rad]
b0=-5; b0=b0*(pi/180); % angle of velocity wrt hor. [deg] neg.=clockwise
v0=6; % velocity of CoM [m/s]

ys0=ls0*sin(a0); % y-comp. of resting spring length [m]

x0=0; % x due to spring angle at initial contact
y0=ls0; % y due to spring angle at initial contact
dx0=v0*cos(b0); % initial x-velocity [m/s]
dy0=v0*sin(b0); % initial y-velocity [m/s]

%pre-allocate memory
tn=[t0];
dynN=[x0 y0 dx0 dy0];
FsN=[0];
aN=[0];
ien=[];
lsn=[ls0];
```

```
Xgcp=zeros(steps+1,1);

% error check
if y0<=ys0
    msg = 'Variable "y0" must be larger than variable "ys0". Start model in air.';
    error(msg)
    pause
end
%% Simulation
% looping through ODE solvers using different diff. eq. for each phase
% switch is initiated by Event Location functions
for s=1:steps
yn0=[x0; y0; dx0; dy0]; % initial conditions in vector
tspan=[t0 tend]; % time span in vector
options=odeset('Events',@(t,yn) AtoC(t,yn,ls0,ain(s))); % call to event location function
[t,dyn, , , ] = ode45(@(t,yn) aerial(t,yn,g),tspan,yn0,options); % solve until event

xgcp=dyn(end,1)+abs(ls0*cos(ain(s))); Xgcp(s+1)=xgcp; % calculate and add current xgcp ...
    to array
F0n=zeros(length(dyn(:,1)),1); % save *nul* force for power calc.
an=zeros(length(dyn(:,1)),1); % save *nul* angle for force calc.

tn=[tn; t(2:end)]; % append run time
dynN=[dynN; dyn(2:end,:)]; % append states
FsN=[FsN; F0n(3:end)]; % append spring forces
aN=[aN; an(3:end)]; % append leg angles
ie=length(tn); ien=[ien; ie]; % memorise and append event index
lsn=[lsn; repmat(ls0,length(t)-1,1)]; % append current spring length

% end conditions are new initial conditions
x0=dyn(end,1);
y0=dyn(end,2);
dx0=dyn(end,3);
dy0=dyn(end,4);
% end time is new initial time
t0=t(end);

% repeat for contact phase
yn0=[x0; y0; dx0; dy0];
tspan=[t0 tend];
options=odeset('Events',@(t,yn) CtoA(t,yn,ls0,xgcp));
[t,dyn, , , ] = ode45(@(t,yn) contact(t,yn,k,m,g,ls0,xgcp),tspan,yn0,options);

xloc=dyn(1:end,1)-xgcp; % local x-position [m]
cls=sqrt(xloc(1:end).^2+dyn(1:end,2).^2); % current spring length [m]
Fsn=k*(repmat(ls0,length(dyn(:,1)),1)-cls); % save spring force for power calc. [N]
an=atan(dyn(:,2)./xloc); % leg angle during contact [rad]

tn=[tn; t(2:end)];
dynN=[dynN; dyn(2:end,:)];
FsN=[FsN; Fsn(1:end)];
aN=[aN; an(1:end)];
ie=length(tn); ien=[ien; ie];
lsn=[lsn; cls(2:end)];

x0=dyn(end,1);
y0=dyn(end,2);
dx0=dyn(end,3);
dy0=dyn(end,4);
t0=t(end);

% break statement if runner has passed finish
if x0>=xend
    break
end
end
%% Post processing

T=tn; % time vector
X=dynN(:,1); % x-position CoM
Y=dynN(:,2); % y-position CoM
```

```
114 DX=dynN(:,3); % x-velocity CoM
115 DY=dynN(:,4); % y-velocity CoM
```

```
1  function dyn = contact(t,yn,k,m,g,ls0,xgcp)
2  % Govert van der Gun, #4512235
3  % equations of motion contact phase - 2DOF
4
5  x = yn(1);
6  y = yn(2);
7  dx = yn(3);
8  dy = yn(4);
9
10 xloc=x-xgcp; % local x-position [m]
11
12 % leg angle alpha [rad]
13 if xloc<0 % true if x-pos CoM before xgcp
14     a=atan(y/xloc)+pi;
15 elseif xloc==0 % true if x-pos CoM equals xgcp
16     a=0.5*pi;
17 elseif xloc>0 % true if x-pos CoM after xgcp
18     a=atan(y/xloc);
19 end
20
21 ls=sqrt(y^2+xloc^2); % spring length [m]
22
23 ddx=k/m*(ls0-ls)*cos(a);
24 ddy=k/m*(ls0-ls)*sin(a)-g;
25
26 dyn=[dx; dy; ddx; ddy];
27 end
```

```
1  function dyn = aerial(t,yn,g)
2  % Govert van der Gun, #4512235
3  % equations of motion aerial phase - 2DOF
4
5  x = yn(1);
6  y = yn(2);
7  dx = yn(3);
8  dy = yn(4);
9
10 ddx=0;
11 ddy=-g;
12
13 dyn=[dx; dy; ddx; ddy];
14 end
```

```
1  function [position,isterminal,direction] = AtoC(t,yn,ls0,ai)
2  % Govert van der Gun, #4512235
3  % Event location function, forces ODE termination
4
5  x = yn(1);
6  y = yn(2);
7  dx = yn(3);
8  dy = yn(4);
9
10 h=y-ls0*sin(ai); % remaining height h untill h=0
11
12 position = h; % if zero than:
13 isterminal = 1;  % halt integration
14 direction = -1;   % can be approached from positive dir. only
15 end
```

```
1  function [position,isterminal,direction] = CtoA(t,yn,ls0,xgcp)
```

```
2  % Govert van der Gun, #4512235
3  % Event location function, forces ODE termination
4
5  x = yn(1);
6  y = yn(2);
7  dx = yn(3);
8  dy = yn(4);
9
10 xloc=x-xgcp; % local x-position [m]
11 ls=sqrt(y^2+xloc^2); % spring length [m]
12 rsl=ls0-ls; % remaining spring length untill ls0
13
14 position = rsl; % if zero than:
15 isterminal = 1;  % halt integration
16 direction = 0;   % event function can be approached from either direction
17 end
```

C.2. ASLIP Model

```
% Govert van der Gun, #4512235
% RUNME ACTIVE SLIP - 2DOF - ODE

clc
clearvars
close all

% constant properties of the body, spring and actuator
m=75; % mass of body in [kg]
g=9.81; % gravitational force field [N/kg]
lcm=1.00; % height of CoM Levi [m]
ls0=0.4; % resting spring length [m] (measured from Levi = 0.4m)
lamax=lcm-ls0; % max actuator length [m]
lamin=lamax*0.75; % min actuator length [m] (ratio measured from Powell = 1/.45)
k=30; k=k*10000; % stiffness in [N/m]
Cd=1; % ave. drag coefficient of person standing upright
rho=1.225; % air density [kg/m^3]
A=0.65; % frontal area of person standing upright (tight clothing) [m^2]

% variable pre-determined properties:
% actuator force in [BW]
Fa=[2; repmat(1.7,5,1); repmat(1.6,4,1);
       repmat(1.5,50,1)]; Fa=Fa*m*g;

% initial contact angels [deg] measured from raw (Levi)
ain=[101; 102; 103; 104; 105; 106; 107; 108; 109; 110;
     110; 111; 111; 112; 112; 113; 113; 114; 114; 115;
     115; 116; 116; 117; 117; 118; 118; 119; 119; 120;
     repmat(120,10,1);
     120; 120; 119; 119; 119; 118; 118; 118; 117; 117;
     117; 116; 116; 116; 115; 115; 114; 114; 113; 113]; ain=ain.*pi/180;

% actuator force angles [deg]
afn=[60; 70; 75; repmat(80,22,1); repmat(85,15,1); repmat(90,20,1)]; afn=afn.*pi/180;
%% Pre-processing
global xgcp % declare global value xgcp to be used across all functions

% Running time
t0=0; % start time [s]
tend=25; % maximum time to simulate [s]
xend=100; % maximum distance to simulate in [m]
steps=55; % maximum number of steps to simulate [-]

% Initial conditions
xgcp=0; % initial x-position of Ground Contact Point [m]
a0=afn(1); % inital leg angle [rad]
cls=ls0-(Fa(1)/k); % initial compression of spring due to Fa [m]
cla=lamin; % initial actuator length [m]

x0=(cls+lamin)*cos(a0); % initial x-position [m]
y0=(cls+lamin)*sin(a0); % initial y-position [m]
dx0=0; % initial x-velocity [m/s]
dy0=0; % initial y-velocity [m/s]

%pre-allocate memory
tn=[t0];
dynN=[x0 y0 dx0 dy0];
FaN=[Fa(1)];
FsN=[0];
ten=[];
yen=[];
ien=[];
lsn=[cls];
lan=[cla];
Xgcp=zeros(steps+1,1);
%% Simulation
% looping through ODE solvers using different diff. eq. for each phase
```

```
% switch is initiated by Event Location functions
for s=1:steps
yn0=[x0; y0; dx0; dy0]; % initial conditions in vector
tspan=[t0 tend]; % time span in vector
options=odeset('Events',@(t,yn) CAtoCP(t,yn,cls(end),lamax)); % call to event location ...
    function
[t,dyn,te,ye,] = ode45(@(t,yn) ...
    contactA(t,yn,Fa(s),m,g,afn(s),rho,Cd,A),tspan,yn0,options); % solve until event

xloc=dyn(1:end,1)-xgcp; % local x-position [m]
cla=sqrt(xloc(1:end).^2+dyn(1:end,2).^2)-cls(end); % current actuator length
Fan=repmat(Fa(s),length(dyn(:,1)),1); % save actuator force for power calc.
F0n=zeros(length(dyn(:,1)),1); % save *nul* force for power calc.

tn=[tn; t(2:end)]; % append run time
dynN=[dynN; dyn(2:end,:)]; % append states
FaN=[FaN; Fan(2:end)]; % append actuator forces
FsN=[FsN; F0n(2:end)]; % append actuator forces
ten=[ten; te]; % append event times
yen=[yen; ye]; % append event states
ie=length(tn); ien=[ien; ie]; % memorise and append event index
lsn=[lsn; repmat(cls(end),length(t)-1,1)]; % append current spring length
lan=[lan; cla(2:end)]; % append current actuator length

% end conditions are new initial conditions
x0=dyn(end,1);
y0=dyn(end,2);
dx0=dyn(end,3);
dy0=dyn(end,4);
% end time is new initial time
t0=t(end);

% repeat for passive contact phase 2
yn0=[x0; y0; dx0; dy0];
tspan=[t0 tend];
options=odeset('Events',@(t,yn) CPtoA(t,yn,lamax,ls0));
[t,dyn,te,ye,] = ode45(@(t,yn) ...
    contactP(t,yn,k,m,g,ls0,cla(end),rho,Cd,A),tspan,yn0,options);

xloc=dyn(1:end,1)-xgcp; % local x-position [m]
cls=sqrt(xloc(1:end).^2+dyn(1:end,2).^2)-cla(end); % current spring length
Fsn=k*(repmat(ls0,length(dyn(:,1)),1)-cls); % save spring force for power calc.
F0n=zeros(length(dyn(:,1)),1); % save *nul* force for power calc.

tn=[tn; t(2:end)];
dynN=[dynN; dyn(2:end,:)];
FaN=[FaN; F0n(2:end)];
FsN=[FsN; Fsn(2:end)];
ten=[ten; te];
yen=[yen; ye];
ie=length(tn); ien=[ien; ie];
lsn=[lsn; cls(2:end)];
lan=[lan; repmat(cla(end),length(t)-1,1)]; cla=lamin; % reset actuator length

x0=dyn(end,1);
y0=dyn(end,2);
dx0=dyn(end,3);
dy0=dyn(end,4);
t0=t(end);

% repeat for aerial phase
yn0=[x0; y0; dx0; dy0];
tspan=[t0 tend];
options=odeset('Events',@(t,yn) AtoCP(t,yn,lamin,ls0,ain(s)));
[t,dyn,te,ye,] = ode45(@(t,yn) aerial(t,yn,g,m,rho,Cd,A),tspan,yn0,options);

F0n=zeros(length(dyn(:,1)),1); % save *nul* force for power calc.

tn=[tn; t(2:end)];
dynN=[dynN; dyn(2:end,:)];
FaN=[FaN; F0n(2:end)];
```

```
FsN=[FsN; F0n(2:end)];
ten=[ten; te];
yen=[yen; ye];
ie=length(tn); ien=[ien; ie];
lsn=[lsn; repmat(cls(end),length(t)-1,1)];
lan=[lan; repmat(cla,length(t)-1,1)];

x0=dyn(end,1);
y0=dyn(end,2);
dx0=dyn(end,3);
dy0=dyn(end,4);
t0=t(end);

xi=(lamin+ls0)*cos(ain(s)); % determine x at initial contact
xgcp=x0-xi; % determine xgcp
Xgcp(s+1)=xgcp; % add current xgcp to array

% repeat for passive contact phase 1
yn0=[x0; y0; dx0; dy0];
tspan=[t0 tend];
options=odeset('Events',@(t,yn) CPtoCA(t,yn));
[t,dyn,te,ye, ] = ode45(@(t,yn) contactP(t,yn,k,m,g,ls0,cla,rho,Cd,A),tspan,yn0,options);

xloc=dyn(1:end,1)-xgcp; % local x-position [m]
cls=sqrt(xloc(1:end).^2+dyn(1:end,2).^2)-cla; % current spring + actuator length [m]
Fsn=k*(repmat(ls0,length(dyn(:,1)),1)-cls); % save spring force for power calc.
F0n=zeros(length(dyn(:,1)),1); % save *nul* force for power calc.

tn=[tn; t(2:end)];
dynN=[dynN; dyn(2:end,:)];
FaN=[FaN; F0n(2:end)];
FsN=[FsN; Fsn(2:end)];
ten=[ten; te];
yen=[yen; ye];
ie=length(tn); ien=[ien; ie];
lsn=[lsn; cls(2:end)];
lan=[lan; repmat(cla,length(t)-1,1)];

x0=dyn(end,1);
y0=dyn(end,2);
dx0=dyn(end,3);
dy0=dyn(end,4);
t0=t(end);

% break statement if runner has passed finish
if x0>=xend
    break
end
end
%% Post processing
T=tn; % time vector
X=dynN(:,1); % x-position CoM
Y=dynN(:,2); % y-position CoM
DX=dynN(:,3); % x-velocity CoM
DY=dynN(:,4); % y-velocity CoM
```

```
function dyn = contactA(t,yn,Fa,m,g,af,rho,Cd,A)
% Govert van der Gun, #4512235
% equations of motion active contact phase - 2DOF

x = yn(1);
y = yn(2);
dx = yn(3);
dy = yn(4);

Fd=1/2*rho*dx^2*Cd*A; % aerodynamic drag

ddx=Fa/m*cos(af)-Fd/m;
ddy=Fa/m*sin(af)-g;
```

```

dyn=[dx; dy; ddx; ddy];
end
```

```
function dyn = contactP(t,yn,k,m,g,ls0,cal,rho,Cd,A)
% Govert van der Gun, #4512235
% equations of motion passive contact phase - 2DOF
global xgcp

x = yn(1);
y = yn(2);
dx = yn(3);
dy = yn(4);

Fd=1/2*rho*dx^2*Cd*A; % aerodynamic drag

xloc=x-xgcp; % local x-position [m]

% leg angle alpha [rad]
if xloc<0 % true if x-pos CoM before xgcp
    a=atan(y/xloc)+pi;
elseif xloc==0 % true if x6-pos CoM equals xgcp
    a=0.5*pi;
elseif xloc>0 % true if x-pos CoM after xgcp
    a=atan(y/xloc);
end

ls=sqrt(y^2+xloc^2)-cal; % spring length [m]

ddx=k/m*(ls0-ls)*cos(a)-Fd/m;
ddy=k/m*(ls0-ls)*sin(a)-g;

dyn=[dx; dy; ddx; ddy];
end
```

```
function dyn = aerial(t,yn,g,m,rho,Cd,A)
% Govert van der Gun, #4512235
% equations of motion aerial phase - 2DOF

x = yn(1);
y = yn(2);
dx = yn(3);
dy = yn(4);

Fd=1/2*rho*dx^2*Cd*A; % aerodynamic drag

ddx=-Fd/m;
ddy=-g;

dyn=[dx; dy; ddx; ddy];
end
```

```
function [position,isterminal,direction] = AtoCP(t,yn,lamin,ls0,ai)
% Govert van der Gun, #4512235
% Event location function, forces ODE termination

x = yn(1);
y = yn(2);
dx = yn(3);
dy = yn(4);

h=y-(lamin+ls0)*sin(ai); % remaining height h untill h=0

position = h; % if zero than:
isterminal = 1;  % halt integration
```

```
direction = -1;   % can be approached from either direction
end
```

```
function [position,isterminal,direction] = CPtoA(t,yn,lamax,ls0)
% Govert van der Gun, #4512235
% Event location function, forces ODE termination
global xgcp

x = yn(1);
y = yn(2);
dx = yn(3);
dy = yn(4);

xloc=x-xgcp; % local x-position [m]
ls=sqrt(y^2+xloc^2)-lamax; % spring length [m]
rsl=ls0-ls; % remaining spring length untill ls0

position = rsl; % if zero than:
isterminal = 1;  % halt integration
direction = -1;   % event function must be decreasing
end
```

```
function [position,isterminal,direction] = CAtoCP(t,yn,lsn,lamax)
% Govert van der Gun, #4512235
% Event location function, forces ODE termination
global xgcp

x = yn(1);
y = yn(2);
dx = yn(3);
dy = yn(4);

xloc=x-xgcp; % local x-position [m]
rla=sqrt(y^2+xloc^2)-lsn-lamax; % remaining length la until lamax

position = rla; % if zero than:
isterminal = 1;  % halt integration
direction = 0;   % can be approached from either direction
end
```

```
function [position,isterminal,direction] = CPtoCA(t,yn)
% Govert van der Gun, #4512235
% Event location function, forces ODE termination

x = yn(1);
y = yn(2);
dx = yn(3);
dy = yn(4);

position = dy; % if zero than:
isterminal = 1;  % halt integration
direction = 1;   % event function must be increasing
end
```

C.3. Optimisation

```
% Run file for optmisation of RUNME ODE
% Govert van der Gun, 4512235

% the functions RMsimu and RMeval that are called to in this script are
% basically the same as the ASLIP RUNME file.

clc
close all
clearvars

%% Fixed parameters

% constant properties of the body, spring and actuator
m=75; % mass of body in [kg]
g=9.81; % gravitational force field [N/kg]
lcm=1.00; % height of CoM Levi [m]
ls0=0.4; % resting spring length [m] (measured from Levi = 0.4m)
lamax=lcm-ls0; % max actuator length [m]
lamin=lamax*0.75; % min actuator length [m] (ratio measured from Powell = 1/.45)
Cd=1; % ave. drag coefficient of person standing upright
rho=1.225; % air density [kg/m^3]
A=0.65; % frontal area of person standing upright (tight clothing) [m^2]

con=[m; g; ls0; lamax; lamin; Cd; rho; A];

% pre-determined physiological properties:
% actuator force in [BW]
Fa=[2; repmat(1.7,5,1); repmat(1.6,4,1);
       repmat(1.5,50,1)]; Fa=Fa*m*g;

% initial contact angels [deg] measured from raw (Levi)
ain=[101; 102; 103; 104; 105; 106; 107; 108; 109; 110;
     110; 111; 111; 112; 112; 113; 113; 114; 114; 115;
     115; 116; 116; 117; 117; 118; 118; 119; 119; 120;
     repmat(120,10,1);
     120; 120; 119; 119; 119; 118; 118; 118; 117; 117;
     117; 116; 116; 116; 115; 115; 114; 114; 113; 113]; ain=ain.*pi/180;

% actuator force angles [deg]
afn=[60; 70; 75; repmat(80,22,1); repmat(85,15,1); repmat(90,20,1)]; afn=afn.*pi/180;
%% Initial Conditions & simulation parameters
global xgcp

% Initial conditions
xgcp=0; % initial x-position of Ground Contact Point [m]
dx0=0; % initial x-velocity [m/s]
dy0=0; % initial y-velocity [m/s]

init=[xgcp; dx0; dy0];

% Simulation parameters
t0=0; % start time [s]
tend=20; % maximum time to simulate [s]
xend=100; % maximum distance to simulate in [m]
steps=60; % maximum number of steps to simulate [-]

simpar=[t0; tend; xend; steps];
%% Optimalisation

% initial guess of free variables
% stiffness in [N/m]
K0=[30; 30; 30; 30; 30; 30]; K0=K0.*1e3; % starting stiffness
Kmin=[24; 24; 24; 24; 24; 24]; Kmin=Kmin.*1e3; % lower bound stiffness
Kmax=[36; 36; 36; 36; 36; 36]; Kmax=Kmax.*1e3; % upper bound stiffness
lk=length(K0); % amount of stiffnesses
spk=steps/lk; % how many steps per k value

```

```
68 % group starting points and constraints of inputs/free variables
69 est0=[K0]; % initial guess
70 min0=[Kmin]; % bounds min
71 max0=[Kmax]; % bounds max
72 len=[lk; spk]; % lengths and steps per input (if less inputs than steps)
73
74 % optimisation algorithm and options
75 tic
76 fcn=@(inp) RMsimu(inp,Fa,afn,ain,len,con,init,simpar); % set criterion function
77 options = optimoptions('patternsearch','UseParallel',true,'UseCompletePoll',true,...
78             'UseVectorized',false,'MeshTolerance',1e-6);
79 optim=patternsearch(fcn,est0,[],[],[],[],min0,max0); % run optimalisation with input ...
       parameters
80 toc
81 %% Evaluation
82 % seperate optimised variables
83 Kopt=optim(1:lk);
84
85 % evaluate outcome with found optimum (for plotting)
86 [tn,dynN,ien,yen,F,L,Xgcp]=RMeval(Kopt,Fa,afn,ain,len,con,init,simpar);
87
88 % remove variables that are not used in optimisation
89 s=ceil(length(ien)/4); % amount of steps taken by model
90 iopt=[ceil(s/spk)]; % index of the lst optimised inputs
91 Kopt=Kopt(1:iopt(1)); % limit optim. vectors to the last optimised value
92
93 % display results
94 % find first index were X is great or equal than xend
95 ifin=find(dynN(:,1)>=xend,1,'first');
96 if dynN(end,1)>=xend && all(dynN(1:ifin,2)>0) % athlete has finished (no y<0 and x>100)
97     Tfin=tn(ifin); % finish time is time at this index
98     fprintf('The finish time is %.3f s with phase-specific (every %d steps) stiffness: ...
           \n',Tfin,spk);
99     Kopt
100 else % athlete has not finished
101     ifin=length(dynN); % ifin is the max length of results
102     disp('Athlete did not finish. Try different initial conditions');
103 end
104 %% Post processing
105 T=tn; % time vector
106 X=dynN(:,1); % x-position CoM
107 Y=dynN(:,2); % y-position CoM
108 DX=dynN(:,3); % x-velocity CoM
109 DY=dynN(:,4); % y-velocity CoM
```

Bibliography

[1] Souhaiel M Chelly and Christian Denis. Leg power and hopping stiffness: relationship with sprint running performance. *Medicine & Science in Sports & Exercise*, 33(2):326–333, 2001.

[2] Claire T Farley and Octavio Gonzalez. Leg stiffness and stride frequency in human running. *Journal of biomechanics*, 29(2):181–186, 1996.

[3] Hiroaki Hobara, Brian S Baum, Hyun Joon Kwon, and Jae Kun Shim. Running mechanics in amputee runners using running-specific prostheses. *Japanese Journal of Biomechanics in Sports and Exercise*, 17(1):1–9, 2013.

[4] Hiroaki Hobara, Shuichi Tominaga, Shingo Umezawa, Koudai Iwashita, Atsuo Okino, Taku Saito, Fumio Usui, and Toru Ogata. Leg stiffness and sprint ability in amputee sprinters. *Prosthetics and orthotics international*, 36(3):312–317, 2012.

[5] Peter G Weyand, Deborah B Sternlight, Matthew J Bellizzi, and Seth Wright. Faster top running speeds are achieved with greater ground forces not more rapid leg movements. *Journal of applied physiology*, 89(5):1991–1999, 2000.

[6] International Paralympic Committee. *Athletics Rules and Regulations 2016-2017*, 2016.

[7] Reinhard Blickhan. The spring-mass model for running and hopping. *Journal of biomechanics*, 22(11-12):1217–1227, 1989.

[8] Lara Grobler, Suzanne Ferreira, and Elmarie Terblanche. Paralympic sprint performance between 1992 and 2012. *International journal of sports physiology and performance*, 10(8):1052–1054, 2015.

[9] Hossein Hassani, Mansi Ghodsi, Mehran Shadi, Siamak Noroozi, and Bryce Dyer. An overview of the running performance of athletes with lower-limb amputation at the paralympic games 2004–2012. *Sports*, 3(2):103–115, 2015.

[10] Hiroaki Hobara, Yoshiyuki Kobayashi, Thijs A Heldoorn, and Masaaki Mochimaru. The fastest sprinter in 2068 has an artificial limb? *Prosthetics and orthotics international*, page 0309364614564026, 2015.

[11] Sheila A Dugan and Krishna P Bhat. Biomechanics and analysis of running gait. *Physical Medicine and Rehabilitation Clinics*, 16(3):603–621, 2005.

[12] Steffen Willwacher, Volker Herrmann, Kai Heinrich, Johannes Funken, Wolfgang Potthast, Ian Bezodis, Gerda Strutzenberger, Gareth Irwin, and GertPeter Brüggemann. Sprint start kinetics: Comparison of amputee and non-amputee sprinters. In *ISBS-Conference Proceedings Archive*, volume 33, 2016.

[13] Paolo Taboga, Alena M Grabowski, Pietro Enrico di Prampero, and Rodger Kram. Optimal starting block configuration in sprint running: A comparison of biological and prosthetic legs. *Journal of applied biomechanics*, 30(3):381–389, 2014.

[14] Maćkała Krzysztof and Antti Mero. A kinematics analysis of three best 100 m performances ever. *Journal of human kinetics*, 36(1):149–160, 2013.

[15] Peter G Weyand, Matthew W Bundle, Craig P McGowan, Alena Grabowski, Mary Beth Brown, Rodger Kram, and Hugh Herr. The fastest runner on artificial legs: different limbs, similar function? *Journal of Applied Physiology*, 107(3):903–911, 2009.

[16] Hiroaki Hobara, Brian S Baum, Hyun-Joon Kwon, Ross H Miller, Toru Ogata, Yoon Hyuk Kim, and Jae Kun Shim. Amputee locomotion: Spring-like leg behavior and stiffness regulation using running-specific prostheses. *Journal of biomechanics*, 46(14):2483–2489, 2013.

[17] Andrea Monte, Valentina Muollo, Francesca Nardello, and Paola Zamparo. Sprint running: how changes in step frequency affect running mechanics and leg spring behaviour at maximal speed. *Journal of sports sciences*, 35(4):339–345, 2017.

[18] H Hobara, Y Sano, Y Kobayashi, TA Heldoorn, and M Mochimaru. Step frequency and step length of 200-m sprint in able-bodied and amputee sprinters. *International journal of sports medicine*, 95 (02):165–168, 2015.

[19] H Hobara, Y Kobayashi, and M Mochimaru. Spatiotemporal variables of able-bodied and amputee sprinters in men's 100-m sprint. *International journal of sports medicine*, 36(06):494–497, 2015.

[20] P G Weyand and M W Bundle. Point: artificial legs do make artificially fast running speeds possible. *Journal of Applied Physiology*, 108(4):1011–1012, 2009.

[21] Thomas A McMahon and Peter R Greene. The influence of track compliance on running. *Journal of biomechanics*, 12(12):893–904, 1979.

[22] C. Bret, A. Rahmani, A B Dufour, L. Messonnier, and J R Lacour. Leg strength and stiffness as ability factors in 100 m sprint running. *Journal of Sports Medicine and Physical Fitness*, 42(3):274, 2002.

[23] Laura Charalambous, Gareth Irwin, Ian N Bezodis, and David Kerwin. Lower limb joint kinetics and ankle joint stiffness in the sprint start push-off. *Journal of sports sciences*, 30(1):1–9, 2012.

[24] Adamantios Arampatzis, GertPeter Brüggemann, and Verena Metzler. The effect of speed on leg stiffness and joint kinetics in human running. *Journal of biomechanics*, 32(12):1349–1353, 1999.

[25] Owen N Beck, Paolo Taboga, and Alena M Grabowski. Prosthetic model, but not stiffness or height, affects the metabolic cost of running for athletes with unilateral transtibial amputations. *Journal of Applied Physiology*, 123(1):38–48, 2017.

[26] Gert-Peter Brüggemann, Adamantios Arampatzis, Frank Emrich, and Wolfgang Potthast. Biomechanics of double transtibial amputee sprinting using dedicated sprinting prostheses. *Sports Technology*, 1(4-5):220–227, 2008.

[27] Alena M Grabowski, Craig P McGowan, William J McDermott, Matthew T Beale, Rodger Kram, and Hugh M Herr. Running-specific prostheses limit ground-force during sprinting. *Biology letters*, 6(2):201–204, 2010.

[28] Thomas A McMahon and George C Cheng. The mechanics of running: how does stiffness couple with speed? *Journal of biomechanics*, 23:65–78, 1990.

[29] Andre Seyfarth, Hartmut Geyer, Michael Günther, and Reinhard Blickhan. A movement criterion for running. *Journal of biomechanics*, 35(5):649–655, 2002.

[30] Owen N Beck, Paolo Taboga, and Alena M Grabowski. Characterizing the mechanical properties of running-specific prostheses. *PloS one*, 11(12):e0168298, 2016.

[31] Ralph V Mann. *The Mechanics of Sprinting and Hurdling*. CreateSpace Independent Publishing Platform, 2011.

[32] Joseph P Hunter, Robert N Marshall, and Peter J McNair. External and internal forces in sprint running. *Routledge Handbook of Biomechanics and Human Movement Science*, pages 354–366, 2008.

[33] Krzysztof Mackala. Optimisation of performance through kinematic analysis of the different phases of the 100 metres. *New Studies in Athletics*, 22(2):7, 2007.

[34] Akihiko Murai, Hiroaki Hobara, Satoru Hashizume, Yoshiyuki Kobayashi, and Mitsunori Tada. Can forward dynamics simulation with simple model estimate complex phenomena?: Case study on sprinting using running-specific prosthesis. *ROBOMECH Journal*, 5(1):10, 2018.

[35] Heikki KyrÖlÄinen, Alain Belli, and Paavo V Komi. Biomechanical factors affecting running economy. *Medicine and science in sports and exercise*, 33(8):1330–1337, 2001.

[36] F Kugler and L Janshen. Body position determines propulsive forces in accelerated running. *Journal of biomechanics*, 43(2):343–348, 2010.

[37] Craig P McGowan, Alena M Grabowski, William J McDermott, Hugh M Herr, and Rodger Kram. Leg stiffness of sprinters using running-specific prostheses. *Journal of The Royal Society Interface*, 9(73):1975–1982, 2012.